# 2D materials based Nanoelectronic devices for multifunctional sensors

Shinde Akash Sandesh

A Dissertation Submitted to

Indian Institute of Technology Hyderabad

In Partial Fulfillment of the Requirements for

The Degree of Master of Technology

भारतीय प्रौद्योगिकी संस्थान हैदराबाद

Indian Institute of Technology Hyderabad

Department of Electrical Engineering

June, 2018

# Declaration

I declare that this written submission represents my ideas in my own words, and where others' ideas or words have been included, I have adequately cited and referenced the original sources. I also declare that I have adhered to all principles of academic honesty and integrity and have not misrepresented or fabricated or falsified any idea/data/fact/source in my submission. I understand that any violation of the above will be a cause for disciplinary action by the Institute and can also evoke penal action from the sources that have thus not been properly cited, or from whom proper permission has not been taken when needed.

ShindeA.

Shinde Akash Sandesh

EE16MTECH11012

# Approval Sheet

This thesis entitled "2D materials based Nanoelectronic devices for multifunctional sensors" by Shinde Akash Sandesh is approved for the degree of Master of Technology from IIT Hyderabad.

Dr. Gajendranath Chowdary

Assistant Professor, Electrical Engineering Dept., IITH

Examiner

Dr. Sushmee Badhulika

Associate Professor, Electrical Engineering Dept., IITH

Adviser

Dr. Chinthapenta R Viswanath

Assistant Professor,

Department of Mechanical and Aerospace Engineering, IITH

Chairman

# Acknowledgements

I am deeply indebted to Prof. Dr. Sushmee Badhulika for her inspiration, support and guidance throughout my course here. Her passion and enthusiasm for teaching, sharing her knowledge and motivating students has not only amazed me, but has made an admirer of everyone who has been taught by her. Whenever I have approached her to discuss ideas for my project, or any generic problem, or even something personal, I have always found an eager listener. I'm grateful to her for being very supportive in letting me pursue my interests and encouraging me to learn and read widely. I'm happy to be a part of her lab which offers an excellent environment for research. Her dedication and energy are infectious, and I'm glad I had the opportunity to be her student for 4 semesters. I'm grateful for this opportunity and look forward to continue my interactions with her in future. I would like to express my gratitude to Dr. Parikshit with whom I have had many insightful discussions, which have bettered my understanding of various topics. My other labmates Dr. Vishnu, Madhava, Rinky, Aarthi, Solomon have been a wonderful group to share any research , sport ideas with academic. I would like to thank Aniket and Pratikesh for helping in lab work at night time and also for graphics. I also take this opportunity to thank Professors Dr. Amit Acharya, Dr. Kaushik Nayak, Dr. Ashudeb Datta, Dr. Shishir Kumar who have all made my courses here pleasurable. My thanks also go to all my batch mates who have made the atmosphere in my classes lively and thought provoking. Last, but most importantly, I'm grateful to my parents, brother, and family for their love, blessings and support throughout this endeavor.

Dedicated to

Friends and family.

# Abstract

Conventional electronic devices deal with rigidity and hence lack of flexibility and stretchablity. A research that is rapidly evolving to develop human friendly flexible and stretchable devices for future electronics. A lot of research has been done on fabricating sensors and electronic devices using 2D materials having characteristics like stretchablity, bendability. These nanomaterials can be used for fabrication of photodetectors, temperature, pressure and strain sensors because of their excellent electronic, thermal, mechanical and optical properties.

The second chapter deals with the demonstration of human integrated electronic devices such as RC filters by utilizing flexible capacitor fabricated using few layer $MoS_2$ grown on Al foil via hydrothermal method as electrodes and cellulose paper as a dielectric material. Advantage of using $MoS_2$ on Al foil is the enhanced capacitance upon strain due to the piezoelectric property of few layered $MoS_2$ over monolayer $MoS_2$. Upon application of external strain on capacitor the mathematical operations such as differentiation and integration are observed for different input signal using RC filter circuits. Such a simple technique for fabrication of flexible variable capacitor is a major step ahead in wearable electronics having applications in digital electronics and sensors.

The 2-D nanomaterials possesses great optical properties so can be used for photo detection. The second chapter deals with 2D ZnO/Gr pyro-phototronic diode. Even though 2D ZnO has been utilized for enhanced self-powered sensing by strain modulation due to its piezoelectric property, study on utilizing pyroelectric property of ZnO remains unexplored. For pyroelectric nan generator, temperature difference can be triggered by external light source which does not disrupt the ZnO structure and also avoids the need for physical bending/pressing as in case of piezoelectric nanogenerator. This work represents the first demonstration of fabrication of flexible 2D ZnO/Gr pyro-phototronic diode where the pyro potential generated in the 2D ZnO due to the NIR illumination adds/subtract with the built-in electric field of the heterojunction and modulates the depletion region of the heterojunction thereby enabling bias free operation.

The fourth chapter deals with the application of properties of 2D materials such as flexibility and wear ability and further wirelessly transmitting related information to distant location. In this work, we demonstrate for the first time, the multifunctionality of $MoS_2$ grown on Al foil and further integrated onto eraser substrate to develop smart, low cost pedometer, gesture communication device and breath sensor by measuring physiological parameters such as strain, touch, hydration levels of lungs respectively. The data generated is wirelessly transmitted to the smartphone via Bluetooth and analyzed using dedicated android applications for individual sensing displays the successful demonstration of such low cost multifunctional wireless personal healthcare monitoring system for Internet of Things (IoT) applications is a major step ahead in flexible and wearable electronics.

**Nomenclature**

DI – Deionized

$MoS_2$ – Molybdenum disulfide

IoT – Internet of Things

ZnS – Zinc sulfide

$V_2O_5$ – Vanadium pentoxide

PET - polyethylene terephthalate

PI - Polyimide

UV – Ultraviolet

NIR – Near Infrared

XRD – X-ray diffraction

XPS – X-ray photoelectron spectroscopy

PL - photoluminescence spectroscopy

FESEM – Field Emission Scanning Electron Microscopy

TEM – Transmission Electron Microscopy

FTIR – Fourier Transform Infrared Spectroscopy

IV – current-voltage

CV – capacitance- voltage

TMDs - Transition-Metal Dichalcogenide

RF – Radio frequency

PCBs – Printed Circuit Boards

EQE – External quantum efficiency

CB – Conduction Band

VB – Valence Band

CVD – Chemical Vapor Deposition

PVD – Physical Vapor Deposition

Al – Aluminum

ZnO – Zinc oxide

Gr – Graphene

CMOS – Complementary Metal Oxide Semiconductor

DSO – Digital Storage Oscilloscope

GF – Gauge Factor

E-skin – Electronic Skin

**Contents**

# Chapter 1

# Introduction

A lot of research has been done on fabricating sensors and electronic devices using 2D materials having characteristics like stretchablity, bendability. These nanomaterials can be used for fabrication of photodetectors, temperature, pressure and strain sensors because of their excellent electronic, thermal, mechanical and optical properties. Interactive electronic passive components wherein the properties can be modulated by external stimuli or human interaction are of great interest due to their applications in smart wearable, electronic circuits, sensors and personal health monitoring. There have been reports to enhance the transport properties of electronic devices such as diodes by piezoelectric property which can be further utilized as frequency modulator at circuit level. The commercially available electronic passive components such as resistors and capacitors are planar and hence thus does not find applications in flexible and wearable electronics. Moreover, the values of resistors and capacitors are fixed and cannot be modulated, except for variable resistor and capacitor which requires numerous complex steps for fabrication. To develop a fully flexible electronic circuit all the components should be flexible and can be integrated to substrate of choice. But the use of flexible electronic passive components such as capacitors and resistors whose property can be modulated by means of external strain by piezoelectric property has not been studied yet. Here, we report the fabrication of flexible interactive electronic passive components such as resistor and capacitor with $MoS_2$ on Al foil as electrode for capacitor and cellulose paper as dielectric. Different lengths of $MoS_2$-Al foil were utilized as resistors. Further, the capacitance of the capacitor was varied by external mechanical strain wherein the applied strain not only alters the physical dimensions of the capacitor but also induces additional charges on the $MoS_2$ electrode due to piezoelectric property thereby enhancing the capacitance. This variable capacitor was utilized in frequency modulator wherein different frequencies were generated based on the strain applied. Passive RC filters were demonstrated and change in characteristic such as gain, phase and time constant of the filters were studied upon application of strain.

Further, the fabricated flexible $MoS_2$ capacitor was integrated to human hand and the corresponding frequency modulation with hand movement was studied. To best of our knowledge, this is the first report of flexible $MoS_2$ film as metal electrode for capacitor and utilizing the piezoelectric property of $MoS_2$ for the development of electronic analog circuits such as oscillators, frequency modulators and RC filters.

The 2-D nanomaterials possesses great optical properties so can be used for photo detection. With the increasing interest in flexible and wearable electronics research, developing self-powered external interactive electronic devices has been of great significance. The analog signals for driving the electronic devices can only be electrically modulated and there are only few reports for external modulation of analog signals using piezo and triboelectricity. But the use of Pyroelectricity for external modulation of analog signals and the development of self-powered devices which can be termed as "Pyrotronic devices" remains unexplored. Pyroelectricity depends on polarization of the material which is dependent on temperature difference. The temperature difference can be induced by means of heat, light etc. The temperature difference across the pyroelectric material leads to decrease in the level of spontaneous polarization and thereby decreasing the free charges bound to the material surface. The open circuit condition leads to the free charges to remain at the electrode surface which generates pyroelectric potential. The short circuit condition allows the current between the two polar surfaces of the pyroelectric material. Similarly, reverse electric current flows as the temperature difference starts to decrease which increases the level of spontaneous polarization.In this work, we demonstrate for the first time the fabrication of Gr/ZnO Pyrotronic diode for NIR photodetection and active analog frequency modulator. Pyroelectric polarization potential generated in ZnO due to the generation of pyroelectric charges has been utilized for the generation of short circuit current which enables bias free photodetection. Upon light illumination, pyroelectric polarization induced in ZnO adds/subtracts from barrier potential of Graphene/ZnO heterojunction thereby changing the depletion region width and the junction capacitance associated with it. This capacitance modulation under light illumination was further utilized for frequency modulation in oscillator circuit. To the best of our knowledge, this is the first report on the fabrication of flexible Gr/ZnO based Pyrotronic diode for self-powered photodetection and frequency modulation with flexible substrate.

The properties of 2D materials such as flexibility and wear ability can be used for applications like pedometer, strain sensor etc. and further wirelessly transmitting related information to distant location. Advancements in flexible and wearable electronics have opened up new avenues in personal healthcare development that can monitor the individual physiological parameters continuously or at a regular intervals and thus act as reliable indicators in early disease diagnostics. These existing technologies in health care however rely mostly on use of sophisticated and specialized sensors, instruments and services thereby leading to an increase in the overall cost of healthcare. Moreover, to access these facilities, individual need to visit hospital and clinics which is not only tedious but also costly. There are recent reports on personal health monitoring which utilize physiological parameters of an individual for glucose monitoring through tears, human motion monitoring, breath sensing for lung disease etc. However, there are few reports which utilizes the low cost sensors for multifunctional sensing wherein the data can be wirelessly transmitted to smartphone with a dedicated android application for individual sensing. Hence there is an urgent need for constant personal health monitoring system with wearable sensors which can monitor parameters such as breath, human motion, human steps (pedometer) and the data can be transferred to the smartphone for a convenient read-out. In this work we develop a low cost wireless personal monitoring system using solution processed $MoS_2$ grown on Al foil as an active sensing element with a dedicated android application for multi parameters sensing. The proposed system can be utilized as a pedometer for calculating the number of walking/running steps and the calories burnt, breath sensor for monitoring breath of an individual, and a hand gesture communication sensor for paralyzed patients. Further each system consists of a dedicated android mobile application which receives the sensor data wirelessly through Bluetooth and displays the information regarding distance travelled, velocity, calories burnt for pedometer module, breath count for breath sensor module and action related to a specific gesture for gesture communication sensor module. To the best of author’s knowledge this is the first demonstration of $MoS_2$ grown on Al foil for wireless personal healthcare monitoring IoT system (pedometer, gesture communication and breath sensing) with dedicated Android application for each sensing module.

Further wirelessly transient electronic system has been developed. With the wireless system 2-D sensor can be destroyed from distant location using Android mobile and Arduino.

# Chapter 2

# Flexible substrate based few layer $MoS_2$ electrode for passive electronic Devices.

**Abstract**— This work reports the demonstration of human integrated electronic devices such as RC filters by utilizing flexible capacitor fabricated using few layer $MoS_2$ grown on Al foil via hydrothermal method as electrodes and cellulose paper as a dielectric material. There are no reports of $MoS_2$ on flexible substrate being utilized as capacitor electrode and further applied human interactive devices. Advantage of using $MoS_2$ on Al foil is the enhanced capacitance upon strain due to the piezoelectric property of few layered $MoS_2$ over monolayer $MoS_2$. As the applied strain increases, increase in the capacitance was observed which is systematically explained by piezoelectric property of $MoS_2$, change in physical dimensions and air gap between $MoS_2$-Al foil and cellulose paper. Upon application of external strain the mathematical operations such as differentiation and integration are observed for different input signal using RC filter circuits. Such a simple technique for fabrication of flexible variable capacitor is a major step ahead in wearable electronics having applications in digital electronics and sensors.

## 2.1 Introduction

Interactive electronic passive components wherein the properties can be modulated by external stimuli or human interaction are of great interest due to their applications in smart wearable, electronic circuits, sensors and personal health monitoring [1]. There have been reports to enhance the transport properties of electronic devices such as diodes by piezoelectric property which can be further utilized as frequency modulator at circuit level [2-3]. The commercially available electronic passive components such as resistors and capacitors are planar and hence thus does not find applications in flexible and wearable electronics. Moreover, the values of resistors and capacitors are fixed and cannot be modulated, except for variable resistor and capacitor which requires numerous complex steps for fabrication. To develop a fully flexible electronic circuit all the components should be flexible and can be integrated to substrate of choice. But the use of flexible electronic passive components such as capacitors and resistors whose property can be modulated by means of external strain by piezoelectric property has not been studied yet.

Molybdenum disulphide ($MoS_2$) is a 2D transition metal dichalcogenide (TMDC) wherein one layer of Mo (Molybdenum) atoms is sandwiched between two layers of S (Sulphur) atoms [4]. It is due to the outstanding properties of $MoS_2$ such as mechanically strong, flexible, optically transparent which makes it highly studied 2D material after graphene [5]. Further, mechanical strain can strongly affect the band structure, carrier effective masses, and transport, optical, and magnetic properties of $MoS_2$ via changing the distance between the atoms and also the crystal symmetry [6-7]. Recent studies report that $MoS_2$ with odd number of layers could produce oscillating piezoelectric voltage [8] and current outputs, expands its scope of usage its potential applications in piezotronic and analog applications. There are various methods to synthesize $MoS_2$ such as Chemical Vapor Deposition (CVD), mechanical exfoliation, chemical exfoliation [9]. However, large area growth of $MoS_2$ and direct deposition of $MoS_2$ on flexible substrate using CVD still remains a challenge. In addition, CVD process needs intricate post processing steps which leads to variation in device to device performance. The exfoliation methods of $MoS_2$ results in small yield and also small lateral size which are difficult to integrate in device fabrication [10]. Hence there is a need to develop a solution processed method for direct growth of few layer $MoS_2$ on different flexible substrates. Hydrothermal solution phase synthesis offers the ability to synthesize 2D materials at low temperatures and low cost with distinct morphologies, high phase purity, good controllability and rapid growth rates because of the rapid diffusion processes [11-12]. There are reports for the growth of $MoS_2$ on different flexible substrate for its use in electronic devices such as diodes, FET, sensors and optoelectronics applications [13, 11]. But the use of $MoS_2$ on flexible substrate as an electrode for capacitor remains unexplored.

Another issue in fabricating flexible electronic components such as capacitor is the deposition of dielectric material by means of sputtering or evaporation which requires sophisticated cleanroom environment. Cellulose paper has been widely reported as a dielectric material in fabrication of paper based electronic devices such as in transistors and a wide variety of sensors [14]. The use of cellulose paper as dielectric not only decreases the complexity of the fabrication process but also significantly reduces the overall cost of the device.

Here, we report the fabrication of flexible interactive electronic passive components such as resistor and capacitor with $MoS_2$ on Al foil as electrode for capacitor and cellulose paper as dielectric. Different lengths of $MoS_2$-Al foil were utilized as resistors. Further, the capacitance of the capacitor was varied by external mechanical strain wherein the applied strain not only alters the physical dimensions of the capacitor but also induces additional charges on the $MoS_2$ electrode due to piezoelectric property thereby enhancing the capacitance. Passive RC filters were demonstrated and change in characteristic such as gain, phase and time constant of the filters were studied upon application of strain. To best of our knowledge, this is the first report of flexible $MoS_2$ film as metal electrode for capacitor and utilizing the piezoelectric property of $MoS_2$ for the development of electronic analog circuits RC filters.

## 2.2 Experimental section

Growth of $MoS_2$ on Al foil**:**

Growth of $MoS_2$ on Al foil was performed by process recently reported from our lab. [11] In brief, growth of large area $MoS_2$ on Al foil (3 cm x 3cm) was achieved using hydrothermal process wherein the seed solution was prepared by mixture of sodium molybdate (10mM) and Thiourea (20mM) in deionized (DI) water. The Al foil was dipped in seed solution for 1 hour followed by drying at 80°C for 30 minutes. The nutrient solution was prepared by mixing sodium molybdate (50mM) and Thiourea (100mM) in DI water. The seed coated Al foil and nutrient solution were then transferred to Teflon line autoclave and was maintained at 200°C for 20 hours in oven. The autoclave was allowed to naturally cool down and the $MoS_2$ deposited Al foil was dried at 70°C for 15 minutes.

Fabrication of capacitor

The as obtained $MoS_2$ grown on Al foil was cut into 1 cm x 1cm and was utilized as metal electrode for the capacitor. Cellulose paper (1 cm x 1 cm) was sandwiched between $MoS_2$-Al foil followed by wrapping the entire capacitor by polyimide (PI) tape. Copper tape was utilized as contacts to connect to the external circuitry. Thickness of the cellulose paper is 180 microns and that of Al foil is 10.5 microns. Hence the height of the sensor is ~ 201 microns (top and bottom Al foil and cellulose paper and excluding the effect of air gap). Schematics showing the synthesis of $MoS_2$ on Al foil and fabrication of capacitor is as shown in figure 1

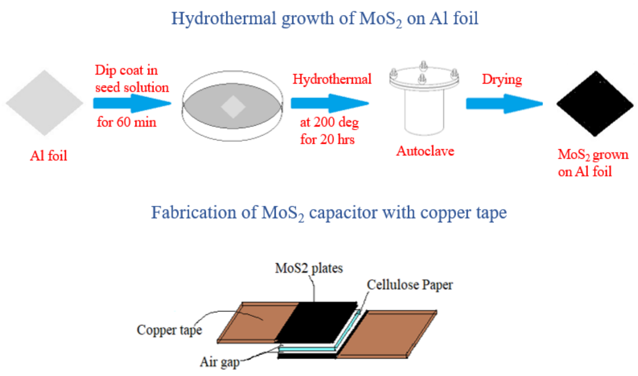


Figure 1: Schematics showing the synthesis of MoS2 on Al foil and fabrication of capacitor using cellulose paper as dielectric

## 2.3 Results and discussions

Flexible electronics aims at fabricating devices wherein the external bending does not affect the performance of the device which is excellent wherein the device can be integrated onto arbitrary curved surface. There are reports wherein there is no change in the performance of monolayer $MoS_2$ devices upon external bending. [15] but there are studies where the external stimuli enhance the performance of few layer $MoS_2$ based electronic devices by modulating the transport properties which opens up new areas of research which can be termed as interactive electronic devices. [16] Hence there is a need for growing few layer $MoS_2$ on flexible substrates whose properties can be modulated upon external strain. In this report, large area few layered $MoS_2$ was grown hydrothermally on Al foil.

XRD analysis of $MoS_2$ deposited on Al foil was performed to study the crystal structure of the grown$MoS_2$ on Al foil as shown in Figure 2a. The characteristic peaks of Al foil noticed at 25°, 35°, 44°, 57° & 61° are the reflections corresponding to (012), (104), (113), (116), (122) planes of Al foil as shown in figure 2b. These peaks correspond to alpha-$Al_2O_3$ which can be ascribed to JCPDS card number 46-1212 [17]. The presence of $MoS_2$ can be confirmed by three signature peaks in XRD spectra at $2\theta = 17.5°$ (002), 33° (100), 58° (110) respectively. The diffraction peaks of $MoS_2$ are marked with ● symbol corresponds to that of hexagonal $MoS_2$ (JCPDS card number. 37-1492) [18]. It can be observed from the XRD pattern that the presence of Al peaks suppresses the diffraction peaks of $MoS_2$ thereby reducing the peak intensities.

To analyze the chemical composition and number of layers of $MoS_2$, raman spectroscopy was performed for $MoS_2$ grown on Al foil. Two peaks namely E12g which is in plane vibration and A1g which is out of plane vibration are observed for $MoS_2$ wherein the frequency difference between the E12g and A1g plane is indicative of the number of layers of MoS2 as shown in figure 2b. [19] As the number of the layers change, redshift and bluseshift is observed for E12g peak and A1g peak respectively. These shifts with the frequency separation is routinely used to identify the number of layers of $MoS_2$. As shown in figure 2b, E12g and A1g are observed at 385 $cm^{-1}$ and 406 $cm^{-1}$ respectively giving the frequency difference of 21 $cm^{-1}$ which suggests that as grown $MoS_2$ on Al foil is trilayer $MoS_2$. [20] Further X-ray photoelectron spectroscopy (XPS) was performed of $MoS_2$ grown on Al substrate wherein peaks corresponding to both 1T and 2H phase were observed as shown in figure. The 1T and 2H phases for $MoS_2$ were present at 228.7, 232.1 eV and 229.6 and 232.8 eV, upon deconvolution of Mo 3d spectra. Also, the deconvoluted S2p peak for $MoS_2$ on Al foil are present at 162 eV and 163 eV corresponding to S 2p3/2 and S 2p1/2 as shown in figure. As can be seen from figure, the density of 2H phase is much more than 1T phase illustrating more semiconducting and piezoelectric behavior of the as grown $MoS_2$.

To study the morphology of as grown $MoS_2$ on Al foil, FESEM studies were performed. Figure 2c shows the low magnification FESEM image of $MoS_2$ grown on Al foil wherein microflower like morphology was observed are due to the self-assembly of individual $MoS_2$ nanoflakes. Figures 2d shows the high magnification image where individual $MoS_2$ nanosheets are visible. The growth of $MoS_2$ on Al foil occurs via self-assembly and nucleation which is explained in a report recently published by our group [11].

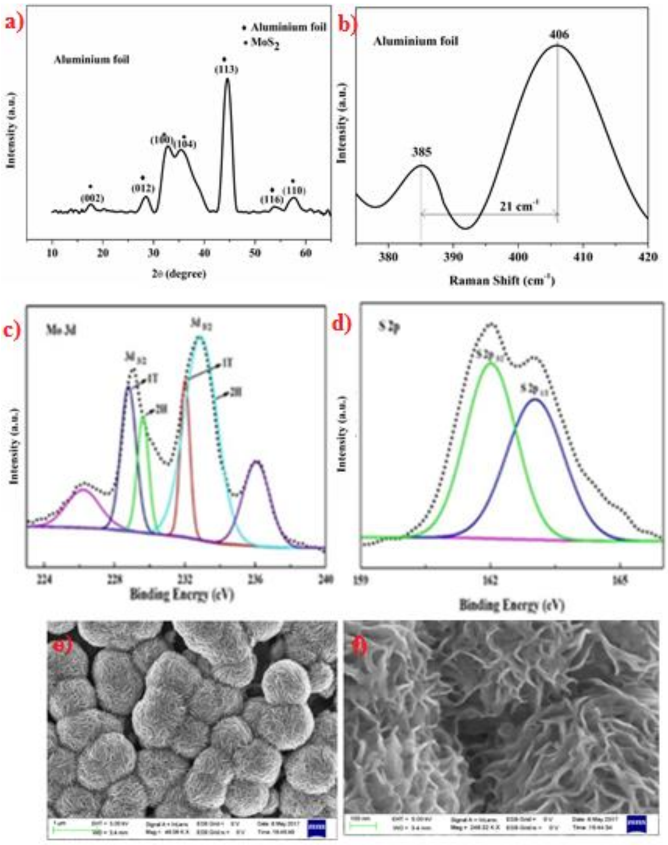


Figure 2: a) XRD of $MoS_2$ grown on Al foil b) Raman spectra of $MoS_2$ grown on Al foil c) a) Mo 3d b) S2p d) Al 2p spectra of MoS2 grown on Aluminum foil e) low magnification FESEM image of $MoS_2$ grown on Al foil f) high magnification FESEM image of $MoS_2$ showing individual $MoS_2$ nanosheets.

The change in the capacitance of flexible $MoS_2$ capacitor after strain can be attributed to three major effects: 1. Change in the physical dimensions of flexible $MoS_2$ capacitor 2. Effect *of* piezoelectric property of $MoS_2$ under strain 3. Effect of air gap between $MoS_2$-Al foil and cellulose paper upon strain

**Change in physical dimensions of flexible $MoS_2$ capacitor upon strain**

For a flexible $MoS_2$ capacitor, cellulose paper has been used as dielectric material sandwiched between $MoS_2$ grown on Al foil. The dielectric constant of the cellulose paper was calculated to be ~ 4.5 which is reported in a recent report from our lab [21]. Copper tape were used as contacts to connect the flexible $MoS_2$ capacitor to external circuitry. When certain amount of external mechanical strain was applied on the $MoS_2$ grown Al foil that act as metal plates, physical dimensions of the flexible $MoS_2$ capacitor changes which results in the increase in the cross section area of the metal plates thereby leading to an increase in the capacitance.

$$C = \frac{\varepsilon A}{d}$$

C = capacitance of the capacitor, A= area of cross section of capacitor, d=distance between the two $MoS_2$ plates (thickness of the paper)

**Effect of piezoelectric property with strain**

Odd layers of $MoS_2$ possess piezoelectric property which induces the charges on $MoS_2$ grown on Al foil when certain external stress is applied. With an odd number of $MoS_2$ atomic layers, the inversion symmetry breaks because of the unpaired odd layered $MoS_2$, resulting in generation of charge(Q) and piezoelectric polarization [8]. Under a tensile strain, positive piezocharges are created at one interface of flexible $MoS_2$ on Al foil, and equivalent negative piezocharges were created at the other interface of $MoS_2$-Al foil. Charges developed on $MoS_2$ grown layers are additive in nature and hence effective charge increases on capacitor.

$$Q = C V$$

Q= charge on the plates of the capacitor, C = capacitance of the capacitor, V = voltage across the capacitor

Therefore at constant voltage operation, with the charge accumulation on the $MoS_2$ based capacitor, the net charge (Q) increases thereby resulting in the enhancement of capacitance. Hence in flexible $MoS_2$ capacitor, due to the piezoelectric property of $MoS_2$ the net capacitance of the flexible $MoS_2$ capacitor further increases. To further verify the generation of charges, strain was applied on pristine $MoS_2$-Al foil with copper tapes at contacts and voltage was measured using oscilloscope. As the strain was applied, maximum of 2Vpp was observed suggesting that MoS2 was capable of generating charges which lead to the increase in capacitance. Graph showing the response of the $MoS_2$-Al under strain can be found in supplementary information (SI) as figure S1. As the $MoS_2$/Al foil is bent inward cyclically to induce the bending strain, corresponding positive voltage peaks can be measured. Bending of $MoS_2$/Al foil leads to create a piezoelectric potential gradient in such a way that one of the contacts would induce positive potential and other will induce negative potential. During such process, the free external charges are driven to the outside circuitry to balance this potential. Similarly, when the strain is released and the $MoS_2$/Al returns to its initial or free-state, the piezoelectric potential diminishes and the free charges that have accumulated at both ends of $MoS_2$/Al foil generates an opposite potential. The free charges gradually flow back in a direction opposite to the accumulation process and hence a negative voltage peak is observed. It should be noted that in this case, the $MoS_2$ grown on Al foil have random crystal orientations wherein Raman spectroscopy studies reveals the growth of trilayer $MoS_2$. There are recent studies on the piezoelectric properties of such few layer solution processed $MoS_2$ with enhanced dielectric and energy storage capacity [22-23]. Further study in terms of physical explanation is needed to fully understand the piezoelectric voltage generation in such systems. In this case, piezoelectric voltage generation upon external strain and increased in the capacitance observed after $MoS_2$ growth on Al foil when compared with pristine Al foil is an indication of piezoelectricity in $MoS_2$.

**Effect of air gap on strain**

Under unstrained conditions of flexible $MoS_2$ capacitor, small air gap exists between the dielectric (cellulose paper) and metal plates ($MoS_2$-Al foil) thereby leading to the formation of virtual capacitance with air as dielectric. Hence there are two capacitances involved, one with dielectric as air ($C_a$) and another with dielectric as cellulose paper ($C_p$) with same area of cross section but different air gaps between the $MoS_2$-Al foil and cellulose paper which results in the series combination of capacitance. It should be noted that the dielectric value of air is less when compared to that of cellulose paper (~ 4.5) and hence the virtual capacitance due to air gap would be less when compared to the capacitance due to cellulose paper. Also, there are air pore visible in the cellulose paper which can be verified from the FESEM image of the pristine cellulose paper and can be found in supplementary information as figure S2. The effect of air pore has been considered while calculating the permittivity of the cellulose paper and hence does not add an extra capacitance. Since both the virtual capacitors are in series combination, the effective capacitance will decrease in unstrained condition and is given by following equation

$$c_{eff} = \frac{c_a c_P}{c_a + c_P}$$

$C_{eff}$ = Effective Capacitance of $MoS_2$ Capacitor, $C_a$= virtual capacitance due to air gap, $C_p$ = capacitance due to cellulose paper

Upon application of external strain to the flexible $MoS_2$ capacitor, the air gap between the cellulose paper and $MoS_2$-Al foil reduces which decreases the virtual capacitance due to the air and hence capacitance due to cellulose paper will become dominant. When large strains are applied where the air gap becomes null, then effective capacitance will consist of capacitance due to cellulose paper ($C_p$) such that virtual capacitance due to air gap ($C_a$) vanishes.

To verify the above effect, experiments were performed on pristine Al foil as capacitor electrodes and cellulose paper as dielectric. It was observed that Al foil with cellulose paper also acts as a capacitor but the capacitance variation upon strain was less when compared to $MoS_2$-Al foil. The variation of capacitance with strain is as shown in figure 3d. For Al foil, under 2% bending strain, 25% increase in capacitance was observed whereas for $MoS_2$-Al, 55% increment in the capacitance was observed which suggests that piezoelectric effect is dominant in case of $MoS_2$-Al foil.

To further explore the flexible $MoS_2$ capacitor in different analog circuits it was applied in RC filters wherein the C of the RC filter was replaced with flexible $MoS_2$ capacitor. The RC filter was tested for both low and high pass filters. Figure 4a shows the circuit diagram of low pass filter (LPF) with both R and C are replaced by flexible $MoS_2$ based resistor and capacitor. The resistance measured for $MoS_2$ resistor was 5.5 MΩ and capacitance of the flexible $MoS_2$ capacitor was measured to 5.2 pF. The cutoff frequency measured was 4.5 KHz. LPF circuit can be defined as the circuit which allows frequencies below a critical frequency, called the *cutoff frequency ($f_{co}$)*, and attenuates the frequencies above the cutoff frequency. Expressions for important parameters of LPF are given as

The gain of the low pass filter is found by

$$\left|H_v(\omega)\right| = \left|\frac{\mathbf{V}_o}{\mathbf{V}_s}\right| = \frac{1}{\sqrt{1+\left(\omega RC\right)^2}}$$

The cut-off frequency of low pass filter is

$$f_{co} = \frac{1}{2\pi RC}$$

The phase difference of low pass filter is

$\phi = -\tan^{-1}(2\pi RC)$

Different inputs were applied to the LPF such as sinusoidal, square and triangular wave and their corresponding output were observed to be inverted cosine, triangular and parabolic nonlinear wave with some attenuation respectively as shown in the figure 4b, c, d. The reactance of a capacitor varies inversely with frequency, while the value of the resistor is independent of frequency. At low frequencies the capacitive reactance of the capacitor will be very large compared to the resistive value of the resistor. Hence the voltage across the flexible $MoS_2$ capacitor will be much larger than the voltage across the flexible $MoS_2$ resistor. Thus at low frequency, upto cut off frequency, output of the LPF will be same as the input signal. At high frequencies the capacitive reactance of the capacitor will be very low compared to the resistive value of the resistor which further decreases as a frequency increases. The voltage across the flexible $MoS_2$ capacitor will be much less than the voltage across the flexible $MoS_2$ resistor. When the input frequency crosses the cut-off frequency of the LPF, the circuit performs the integration of the input wave as seen in figure 4.

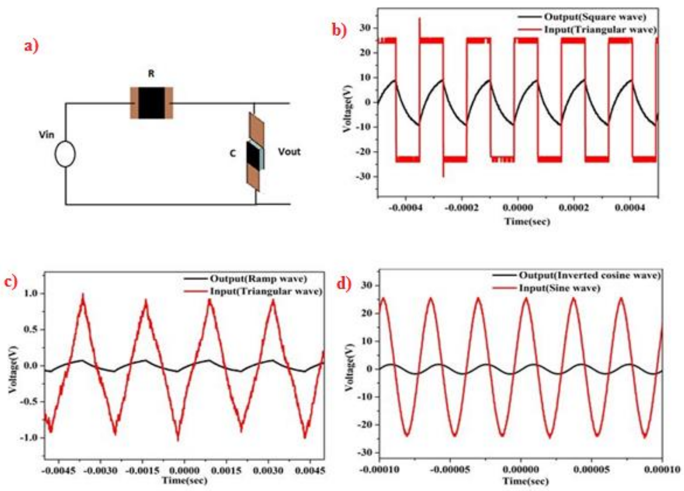


**Figure 4: (a) Circuit Diagram of low pass filter (b) Integration of square wave (c) Integration of triangular wave (d) Integration of sinusoidal wave**

Similarly, high pass filter (HPF) was designed by swapping the positions of R and C. It should be noted that same value R and C were used for HPF design. HPF may be defined as the circuit which passes frequencies above the *critical frequency* ($f_{co}$) but rejects the frequencies below the critical frequency. Expressions for important parameters of HPF are given as

$$|H_n(\omega)| = \left|\frac{V_o}{V_s}\right| = \frac{\omega RC}{\sqrt{1+(\omega RC)^2}}$$

The cut-off frequency of low pass filter is

$$f_{co} = \frac{1}{2\pi RC}$$

The phase difference of low pass filter is

$$\phi = 90^0 - \tan^{-1}(2\pi RC)$$

To test the circuit, similar inputs were applied to the HPF such as sinusoidal, square wave, triangular wave and observed output waveform were cosine, impulse train and square wave with attenuation as shown in the figure 5b, c, d respectively. At high frequencies the capacitive reactance of the flexible $MoS_2$ capacitor will be very low compared to the resistive value of the flexible $MoS_2$ resistor. Thus at high frequency above the cut off frequency output observed was same as the input signal. But, at the low frequencies, the capacitive reactance of the flexible $MoS_2$ capacitor increases compared to the resistive value of the flexible $MoS_2$ resistor which further increases the capacitive reactance as frequency decreases. Hence, voltage across the flexible $MoS_2$ capacitor will be much larger than the voltage across the flexible $MoS_2$ resistor. Thus at the frequencies lower than the cut off frequencies, HPF circuit performs derivative of the input signal as shown in figure 5.

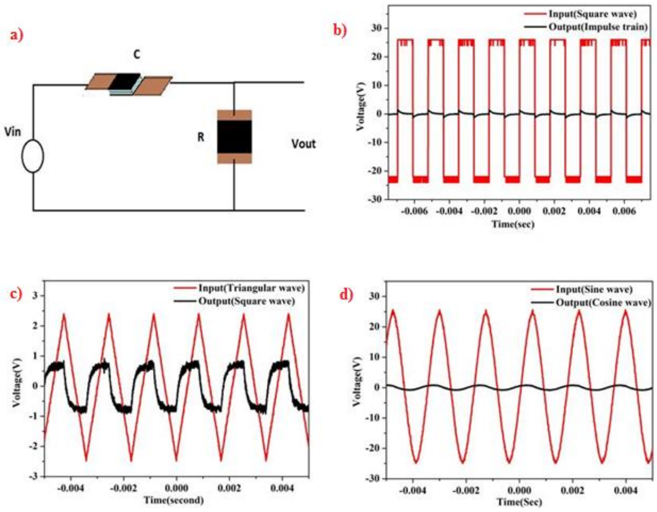


Figure 5: High Pass Filters based on flexible $MoS_2$ capacitor (a) Circuit Diagram of high pass filter (b) Differentiation of square wave (c) Differentiation of triangular wave (d) Differentiation of sinusoidal wave

Further, to study the effect of strain on the performance of HPF, different strains were applied on flexible $MoS_2$ capacitor and the corresponding output were measured. It was observed that capacitance of the flexible $MoS_2$ capacitor increases with applied strain. Hence, in case of HPF (differentiator) application of strain increases results in increase in the flexible $MoS_2$ capacitance and thus capacitive reactance in the circuit decreases. As the reactance of the flexible $MoS_2$ capacitor decreases, the gain of the HPF circuit increases. Next, cut-off frequency is inversely proportional to the capacitance and hence the cut-off frequency of the HPF also decreases. Graph showing the values of the cut-off frequency with different strain can be found in supplementary information as figure S3. The other parameter of the HPF is the phase difference between input and output signal which holds a direct relation with the capacitance as discussed in expressions of HPF circuit and hence upon strain, the phase difference between the input and output signal decreases. Therefore, upon external mechanical strain, the important parameters of the filter circuit such as gain, cut-off frequency and phase can be modulated. Further, time charging and discharging constant ($\tau$ also increases upon application of strain. Figure 6 shows the output of the HPF under different strains for square wave input waveform and their corresponding output signal plot. As can be seen from figure 6, as applied strain increases, output voltage amplitude increases which increases the gain of the HPF. Also the time constant for discharging increases which is due to the increment in the capacitance upon strain.

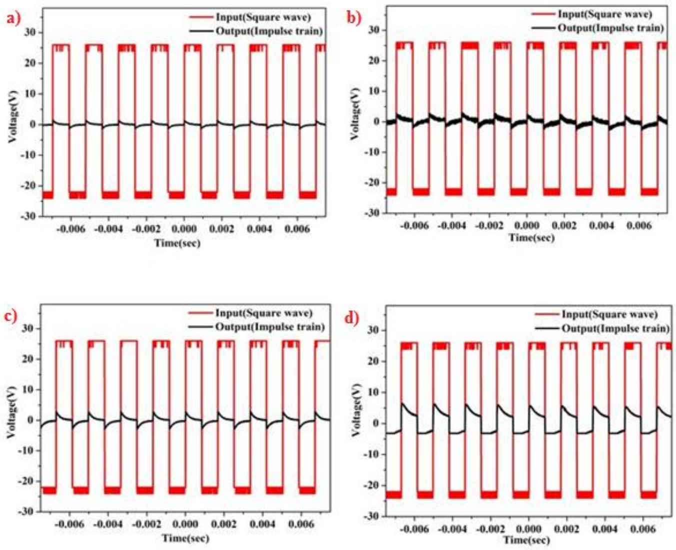


Figure 6) Flexible $MoS_2$ based High Pass Filter under strain (a) Differentiation of square wave without strain (b) Differentiation of square wave with 1% strain (c) Differentiation of square wave with 1.5% strain (d) Differentiation of square wave with 2% strain

There are reports on use of various functional materials for device fabrication wherein external strain modulates the transport properties which could then be utilized for enhancement of the device performance. *Zhang et al.*, reported the fabrication of $MoS_2$/CuO on flexible substrate and strain modulated it for enhancement in photodetector performance [16]. *Sahatiya et al.*, fabricated $MoS_2$/CuO on paper substrate and utilized the strain modulation for designing oscillator circuit [2]. *Zhou et al.*, reported tribotronic tuning of diode for signal modulation [3]. Apart from these, there are various studies which report enhancement in transport properties due to external strain modulation [1, 12,24]. But all of these reports are based on modulating the capacitance of p-n junction by means of complicated cleanroom technology or by solution processed method wherein optimizations are needed to form a uniform junction. There are no reports demonstrating $MoS_2$ as electrode for capacitor material and enhancing the capacitance simply by means of external strain modulation. Cellulose paper was utilized as a dielectric for the fabrication of capacitor which avoids the use of sophisticated cleanroom deposition techniques. Overall cost of each fabricated capacitor is less than $0.02 and. the prototype can be assembled within 2 min.

Moreover, the growth process of $MoS_2$ on Al foil using hydrothermal synthesis is entirely scalable and can be utilized for fabricating large area flexible capacitors.

## 2.4 Conclusion

In summary, we report for the first time, $MoS_2$ on Al foil as electrode and cellulose paper as dielectric for fabrication of flexible capacitor whose capacitance can be modulated upon external mechanical strain and was applied in human integrated electronic passive devices such as filters. As the applied strain increases, increase in the capacitance of flexible MoS2 capacitor was observed. The effect of strain was studied on the filters circuit where the important parameters of the filter circuit such as gain, cut-off frequency, phase and time constant were monitored upon strain. Such a simple and low cost technique for fabrication of flexible and wearable capacitor is a major step ahead in flexible electronics which hold tremendous potential applications in field of analog and digital electronics and sensors for personal healthcare monitoring.

## 2.5 References


1. Sahatiya, P., Jones, S. S., Gomathi, P. T., & Badhulika, S. Flexible substrate based 2D ZnO (n)/graphene (p) rectifying junction as enhanced broadband photodetector using strain modulation. *2D Materials*, vol. 4, pp. 025053, 2017.
2. Sahatiya, P., & Badhulika, S. Fabrication of a solution-processed, highly flexible few layer MoS 2 (n)–CuO (p) piezotronic diode on a paper substrate for an active analog frequency modulator and enhanced broadband photodetector. *Journal of Materials Chemistry C*, **2017**. vol. 44, pp: 11436
3. Zhou, T., Yang, Z. W., Pang, Y., Xu, L., Zhang, C., & Wang, Z. L. Tribotronic tuning diode for active analog signal modulation. *ACS Nano*, **2016**, vol. 11, pp. 882-888.
4. Seifert, G., Terrones, H., Terrones, M., Jungnickel, G., & Frauenheim, T. Structure and electronic properties of MoS 2 nanotubes. *Physical Review Letters*, **2000**, vol. 85, pp. 146.

5. Ataca, C., Sahin, H., Akturk, E., & Ciraci, S. Mechanical and electronic properties of MoS2 nanoribbons and their defects. *The Journal of Physical Chemistry C*, vol. 115, pp. 3934-3941, 2011.
6. Castellanos-Gomez, A., Roldán, R., Cappelluti, E., Buscema, M., Guinea, F., van der Zant, H. S., & Steele, G. A. Local strain engineering in atomically thin MoS2. *Nano Letters*, vol. 13, pp. 5361-5366, 2013.
7. Conley, H. J., Wang, B., Ziegler, J. I., Haglund Jr, R. F., Pantelides, S. T., & Bolotin, K. I. Bandgap engineering of strained monolayer and bilayer MoS2. *Nano Letters*, vol. 13, pp. 3626-3630, 2013.
8. Zhu, H., Wang, Y., Xiao, J., Liu, M., Xiong, S., Wong, Z. J., & Zhang, X. Observation of piezoelectricity in free-standing monolayer MoS2. *Nature Nanotechnology*, vol. 10, pp. 151-155, 2015.
9. Gao, M. R., Xu, Y. F., Jiang, J., & Yu, S. H. Nanostructured metal chalcogenides: synthesis, modification, and applications in energy conversion and storage devices. *Chemical Society Reviews*, vol. 42, pp. 2986-3017, 2013.
10. Coleman, J. N., Lotya, M., O'Neill, A., Bergin, S. D., King, P. J., Khan, U., & Shvets, I. V. Two-dimensional nanosheets produced by liquid exfoliation of layered materials. *Science*, vol. 331, pp. 568-571, 2011.
11. Gomathi, P. T., Sahatiya, P., & Badhulika, S. Large-Area, Flexible Broadband Photodetector Based on ZnS–MoS2 Hybrid on Paper Substrate. *Advanced Functional Materials*, vol. 27, 2017.
12. Sahatiya, P., & Badhulika, S. Strain-modulation-assisted enhanced broadband photodetector based on large-area, flexible, few-layered Gr/MoS2 on cellulose paper. *Nanotechnology*, vol. 28, pp. 455204, 2017.
13. Yin, Z., Li, H., Li, H., Jiang, L., Shi, Y., Sun, Y., & Zhang, H. Single-layer MoS2 phototransistors. *ACS Nano*, vol. 6, pp. 74-80, 2011.
14. Kanaparthi, S., & Badhulika, S. Solvent-free fabrication of a biodegradable all-carbon paper based field effect transistor for human motion detection through strain sensing. *Green Chemistry*, vol. 18, pp. 3640-3646, 2016.
15. Lopez-Sanchez, O., Lembke, D., Kayci, M., Radenovic, A., & Kis, A. Ultrasensitive photodetectors based on monolayer MoS2. *Nature Nanotechnology*, vol. 8, pp. 497-501, 2013.
16. Zhang, K., Peng, M., Wu, W., Guo, J., Gao, G., Liu, Y., & Zhang, Y. A flexible p-CuO/n-MoS 2 heterojunction photodetector with enhanced photoresponse by the piezo-phototronic effect. *Materials Horizons*, vol. 4(2), pp. 274-280, 2017.

17. Sanwaria, A.R., Nagar, M., Bohra, R., Chaudhary, A., Mobin, S.M., Mathur, P. and Choudhary, B.L., Sol–gel synthesis of highly pure α-Al 2 O 3 nano-rods from a new class of precursors of salicylaldehyde-modified aluminum (iii) isopropoxide. Crystal and molecular structure of [Al (OC 6 H 4 CHO) 3], *RSC Advances*, vol. 4, pp. 30081-30089, 2014.
18. Joensen, P., Crozier, E. D., Alberding, N., & Frindt, R. F. A study of single-layer and restacked MoS2 by X-ray diffraction and X-ray absorption spectroscopy. *Journal of Physics C: Solid State Physics*, vol. 20, pp. 4043, 1987.
19. Liu, K. K., Zhang, W., Lee, Y. H., Lin, Y. C., Chang, M. T., Su, C. Y., & Lai, C. S. Growth of large-area and highly crystalline MoS2 thin layers on insulating substrates. *Nano Letters*, vol. 12, pp. 1538-1544, 2012.
20. Mignuzzi, S., Pollard, A. J., Bonini, N., Brennan, B., Gilmore, I. S., Pimenta, M. A., & Roy, D. Effect of disorder on Raman scattering of single-layer MoS2. *Physical Review B*, vol. 91, pp. 195411, 2015.
21. Kanaparthi, S., Sekhar, V. R., & Badhulika, S. Flexible, eco-friendly and highly sensitive paper antenna based electromechanical sensor for wireless human motion detection and structural health monitoring. *Extreme Mechanics Letters*, vol. 9, pp. 324-330, 2016.
22. Jia, Q., Huang, X., Wang, G., Diao, J., & Jiang, P. MoS2 nanosheet superstructures based polymer composites for high-dielectric and electrical energy storage applications. *The Journal of Physical Chemistry C*, vol. 120(19), pp. 10206-10214, 2016.
23. Maity, K., Mahanty, B., Sinha, T. K., Garain, S., Biswas, A., Ghosh, S. K., & Mandal, D. Two-Dimensional Piezoelectric MoS2-Modulated Nanogenerator and Nanosensor Made of Poly (vinlydine Fluoride) Nanofiber Webs for Self-Powered Electronics and Robotics. *Energy Technology*, vol. 5(2), pp. 234-243, 2017.
24. Sahatiya, P., Madhava, C., Shinde, A., & Badhulika, S. (2018). Flexible Substrate Based Few Layer MoS2 Electrode for Passive Electronic Devices and Interactive Frequency Modulation Based on Human Motion. *IEEE Transactions on Nanotechnology*, *17*(2), 338-344

# Chapter 3

# Pyro-phototronic nanogenerator based on flexible 2D ZnO/graphene iheterojunction and its application in self-powered Near Infrared photodetector and active analog frequency modulation


**Abstract**

Even though 2D ZnO has been utilized for enhanced self-powered sensing by strain modulation due to its piezoelectric property, study on utilizing pyroelectric property of ZnO remains unexplored. The piezoelectric property of 2D ZnO works on mechanical strain which disrupts the structure of ZnO leading to the failure of device. For pyroelectric nanogenerator, temperature difference can be triggered by external light source which does not disrupt the ZnO structure and also avoids the need for physical bending/pressing as in case of piezoelectric nanogenerator. This work represents the first demonstration of fabrication of flexible 2D ZnO/Gr pyro-phototronic diode where the pyro potential generated in the 2D ZnO due to the NIR illumination adds/subtract with the built-in electric field of the heterojunction

and modulates the depletion region of the heterojunction thereby enabling bias free operation. Further, the variation in the depletion width of the heterojunction was utilized as a variable capacitor in frequency modulator, wherein, with the increasing intensity, frequency of oscillations increased from 9.8 MHz to 10.42 MHz. The work presented provides an alternative approach for self-powered NIR photodetector and to utilize the same at circuit level having potential applications in the fields of optothermal detections, electronic tuning circuits etc.

## 3.1 Introduction:

With the increasing interest in flexible and wearable electronics research, developing self-powered external interactive electronic devices has been of great significance. The analog signals for driving the electronic devices can only be electrically modulated and there are only few reports for external modulation of analog signals using piezo and triboelectricity. [1-2]But the use of Pyroelectricity for external modulation of analog signals and the development of self-powered devices which can be termed as "Pyrotronic devices" remains unexplored. Pyroelectricity depends on polarization of the material which is dependent on temperature difference. The temperature difference can be induced by means of heat, light etc. The temperature difference across the pyroelectric material leads to decrease in the level of spontaneous polarization and thereby decreasing the free charges bound to the material surface. [3] The open circuit condition leads to the free charges to remain at the electrode surface which generates pyroelectric potential. The short circuit condition allows the current between the two polar surfaces of the pyroelectric material. Similarly, reverse electric current flows as the temperature difference starts to decrease which increases the level of spontaneous polarization.

ZnO, a widely studied n-type metal oxide possesses peculiar electrical, optical and thermal properties which are applied for variety of applications such as field effect transistors, sensors and optoelectronics. [4-5] The piezoelectric property of ZnO has been utilized for fabrication of nanogenerator for energy harvesting. [6] Although many of the ZnO properties and their corresponding applications have been demonstrated but the Pyroelectric property of ZnO remains unexplored for applications in self-powered electronic devices. Hence there is a need to study the pyroelectric property of ZnO for applications like nanogenerator, self-powered photodetectors.

To further expand the scope of application pristine ZnO offers, heterojunction of ZnO have been fabricated with Graphene as p type material which forms heterojunction and hence can be utilized for variety of electronic and optoelectronic applications. [7] There are reports of Gr/ZnO on various flexible substrates such as cellulose paper, eraser, polyimide etc. for enhanced photodetection performance using external strain modulation. [8-10] There are reports of self-powered Gr/ZnO photodetectors on flexible substrate using piezoelectricity property of ZnO. [11-18] But there are no reports of Gr/ZnO self-powered photodetectors utilizing the pyroelectric property of ZnO. The piezoelectric property of ZnO works on mechanical strain on ZnO which disrupts the structure leading to the failure of device. For pyroelectric nanogenerator, temperature difference can be triggered by external light source which does not disrupts the ZnO structure and also avoids the need for physical bending/pressing the device as in case of piezoelectric nanogenerator. Further, every heterojunction exhibits depletion region and junction capacitance. The light induced pyroelectric potential will modulate the barrier potential and hence the junction capacitance modulates. This modulation of the junction capacitance can be utilized for various analog electronic applications such as frequency modulator and oscillator circuits. Even though numerous applications of ZnO have been reported, research along pyroelectric property of ZnO and utilizing it for analog electronic applications remains unexplored.

In this work, we demonstrate for the first time the fabrication of Gr/ZnO Pyrotronic diode for NIR photodetection and active analog frequency modulator. Pyroelectric polarization potential generated in ZnO due to the generation of pyroelectric charges has been utilized for the generation of short circuit current which enables bias free photodetection. Upon light illumination, pyroelectric polarization induced in ZnO adds/subtracts from barrier potential of Graphene/ZnO heterojunction thereby changing the depletion region width and the junction capacitance associated with it. This capacitance modulation under light illumination was further utilized for frequency modulation in oscillator circuit. To the best of our knowledge, this is the first report on the fabrication of flexible Gr/ZnO based Pyrotronic diode for self-powered photodetection and frequency modulation with flexible substrate.

## 3.2 Experimental Section

### *Materials and characterization*

Analytical grade chemicals (Zinc acetate dihydrate, hexamethylenetetramine), ITO coated PET substrates were purchased from Sigma Aldrich. Graphene (8 nm flake size) was procured from Graphene Supermarket, USA. Field Emission Scanning Electron Microscopy (FESEM) analysis was performed by ZEISS Ultra-55 SEM to study morphology. The electrical measurements were carried out with Keithley 4200 SCS instrument. Agilent digital storage oscilloscope (DSO 3062A) was utilized for the measurement of frequency of oscillation of oscillator circuit. NIR source of wavelength 780 nm was utilized for photodetector experiments.

*Growth of ZnO on ITO coated PET substrate*

Hydrothermal synthesis was utilized for the growth of ZnO on ITO coated PET substrate. ITO coated PET substrate was soaked in seed solution consisting of 1mM of Zinc acetate dihydrate [Zn ($CCH_3O_2$). ($H_2O_2$)$_2$] in 10 mL of propanol for 30 minutes followed by drying at 70°C for 30 minutes. The seed deposited ITO-PET substrate was then immersed in nutrient solution consisting of [Zn ($CCH_3O_2$). ($H_2O_2$)$_2$] and hexamethylenetetramine (HMTA) in 1:1concentration. pH of the nutrient solution was adjusted to 10 by dropwise addition of NaOH and hydrothermal was performed at 90°C for 6 hours. The obtained ZnO grown on ITO-PET substrate was dried at 70°C for 30 minutes.

*Fabrication of Graphene/ZnO heterojunction*

Graphene (12 nm flake size procured from Graphene Supermarket) was dispersed in NMP (2 wt. %) and was spin coated on masked ZnO grown ITO-PET and dried in hot air at 90 °C for 1 hour. This was followed by defining contacts on Graphene and ZnO by silver paste. Schematics showing the synthesis and the fabrication procedure is as shown in figure 1.

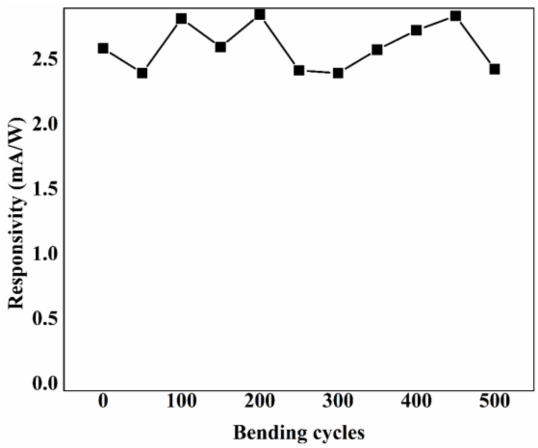


Figure 1: Graph of responsivity v/s bending cycles demonstrating negligible change in the responsivity value

| Material | Voltage | Responsivity | Ref |
|---|---|---|---|
| WSe2 | 2 | 210 mA/W | [R1] |
| Ge | 3 | 16 mA/w | [R2] |
| $MoS_2/ZnS$ | 1 | 4.5 µA/W | [R3] |
| $MoS_2/V_2O_5$ | 1 | 29.4 mA/W | [R4] |
| Graphene/InAs nanowire | Tunable (2-20V) | 0.5 mA/W | [R5] |
| Reduced graphene oxide | 1 | 0.8 A/W | [R6] |
| **Graphene/ZnO** | **0** | **26.4 mA/W** | **This work** |

### 3.3 Results and discussions

Heterojunction (p-n) fabricated using various functional materials are important units in electronics and optoelectronics which finds tremendous applications in Internet of Things (IoT) ranging from health monitoring, security, sensors etc. One such potential application is photodetector where the heterojunction needs to be reversed biased which is conventionally provided by batteries which has issues such as high maintenance cost, limited lifetime and environmental issues. Hence there is a need for self-powered flexible photodetectors which can operate without the need of any external power supply. Emerging field that is recently been explored for self-powered photodetector is pyro-phototronics wherein pyro potential generated is utilized for biasing of the photodetector. [3] But pyro potential generated remains for short duration of time till the temperature difference becomes constant and hence for operation of such self-powered systems time varying field is necessary which can be achieved by constantly turning on and off the light source at regular intervals thereby creating a time varying electric field. This time varying electric field helps in flow of displacement current across the heterojunction which then flows as conduction current through the external circuit. Here, ZnO grown on ITO-PET flexible substrate acts as a pyroelectric material wherein the Near Infrared (NIR) illumination generates temperature difference. The details regarding the growth of 2D ZnO and the fabrication of Graphene/ZnO heterojunction can be found in Supplementary Information. Schematic showing the fabrication procedure is as shown in figure 2.

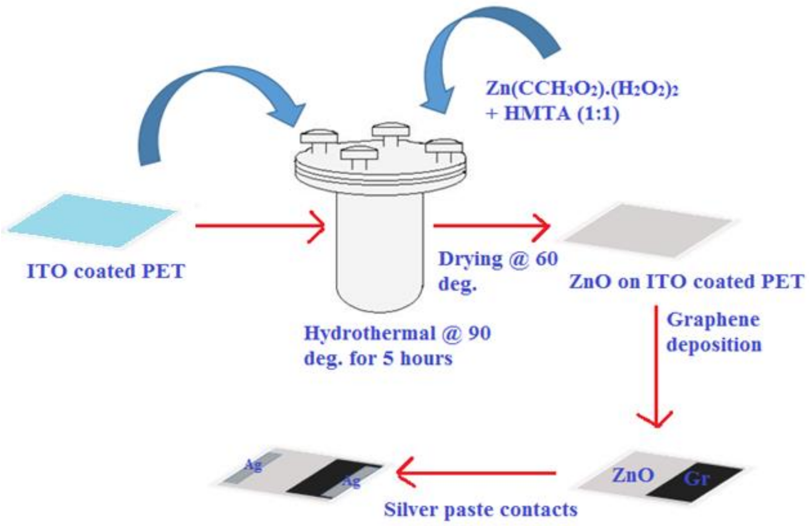


Figure 2: Schematic of the fabrication procedure for Pyrotronic Gr/ZnO diode.

To study the morphology of the as grown ZnO on ITO-PET substrate, detailed FESEM analysis was performed wherein morphology of the 2D ZnO was studied and confirmed. Figure 2a shows the high magnification FESEM image wherein individual 2D ZnO nanosheets are observed wherein the size of 2D ZnO was found to be in sub 200 nm as shown in figure 2b. The growth of 2D ZnO can be attributed to the addition of NaOH wherein the $OH^-$ ions are attracted to the (1000) direction of ZnO which is the natural growth direction and hinders the growth of ZnO in (1000) plane. This results in the growth of ZnO in other two planes leading to the 2D morphology of ZnO as seen in FESEM image in figure 3. Detailed explanation of the growth kinetics and the optimized parameters for the growth of 2D ZnO on flexible substrate can be found in a recent report from our lab [8].

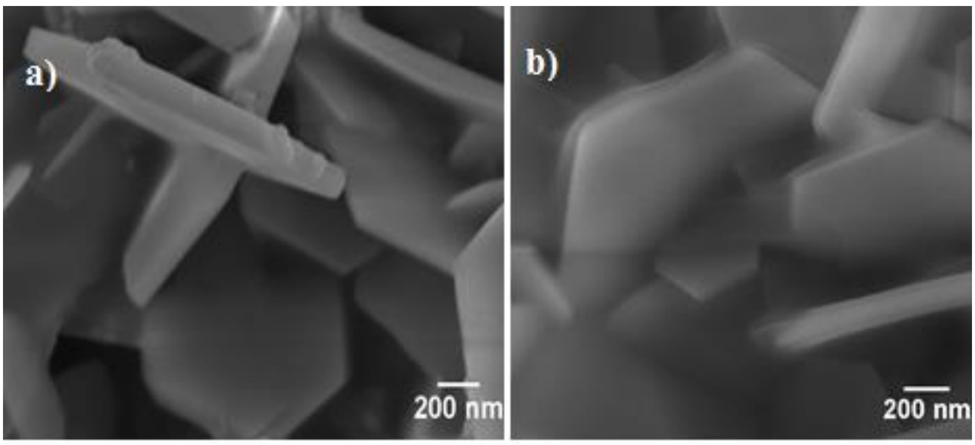


Figure 3: a) High magnification FESEM image demonstrating 2D ZnO Nano flakes morphology b) Few layer transparent 2D ZnO.

To demonstrate the application of the fabricated p-n heterojunction as a self-powered photodetector, I-V characteristics were measured in the range of -1V to 1V with silver paste as contacts. As seen in figure 3a, the graph indicates rectifying junction formation with turnon voltage of 0.47 V. To further study the transport mechanism of Gr/ZnO heterojunction, thermionic emission theory was employed and the ideality factor and barrier height calculated was 1.97 and 0.357 eV which is excellent considering the simplicity of the device fabrication. Expressions for thermionic emission theory and ideality factor calculation can be expressed as

$$I = Io \exp\left(\frac{q(V - IR)}{\eta KT}\right)$$

$$Io = AA^{*}T^{2} exp\left(\frac{-q\Phi_{B}}{KT}\right), A^{*} = \frac{4\pi q m^{*} K^{2}}{h^{3}}$$

$$\eta = \frac{q}{KT}\frac{dV}{d(lnI)}$$

Where K is boltzman constant, R is series resistance and q is electronic charge, T is absolute temperature, A is junction area and A* is Richardson coefficient which is assumed to be 32 for ZnO and m* is the effective mass which is 0.27 m0. ΦB and η are barrier height and ideality factor.

The ideality factor of the fabricated Gr/ZnO heterojunction as found to be greater than 1 which can be attributed to the defects introduced in ZnO during the hydrothermal growth, inhomogeneous growth as evident from FESEM images [12] and presence of surface states. Also, the barrier height of the heterojunction was found to be higher than the work function difference between Gr and ZnO which was due to the possible oxidation of Gr which makes it more p type thereby increasing the barrier height. Figure 3b shows the IV characteristics of the Gr/ZnO under different NIR illuminations wherein increase in current was observed with increasing NIR illumination intensity. It should be noted here that increment in the current is not due to the pyro potential as when the voltage is swept and the current is measured the rate of change of temperature becomes constant which vanishes the pyro potential. Therefore, ZnO film experiences constant temperature and hence the current increment is due to the temperature increase and not due to pyroelectric potential. Also, NIR illumination was only focused on ZnO and not on Graphene. As the intensity of NIR increases, temperature experienced by the ZnO film increases and hence current increases. The increment in the current is due to the decrease in the fermi level of ZnO which decreases the barrier height thereby leading to the increment in current. The schottky barrier height change with different intensities is as shown in figure 4c and as high as 26 meV change in the schottky barrier height was observed.

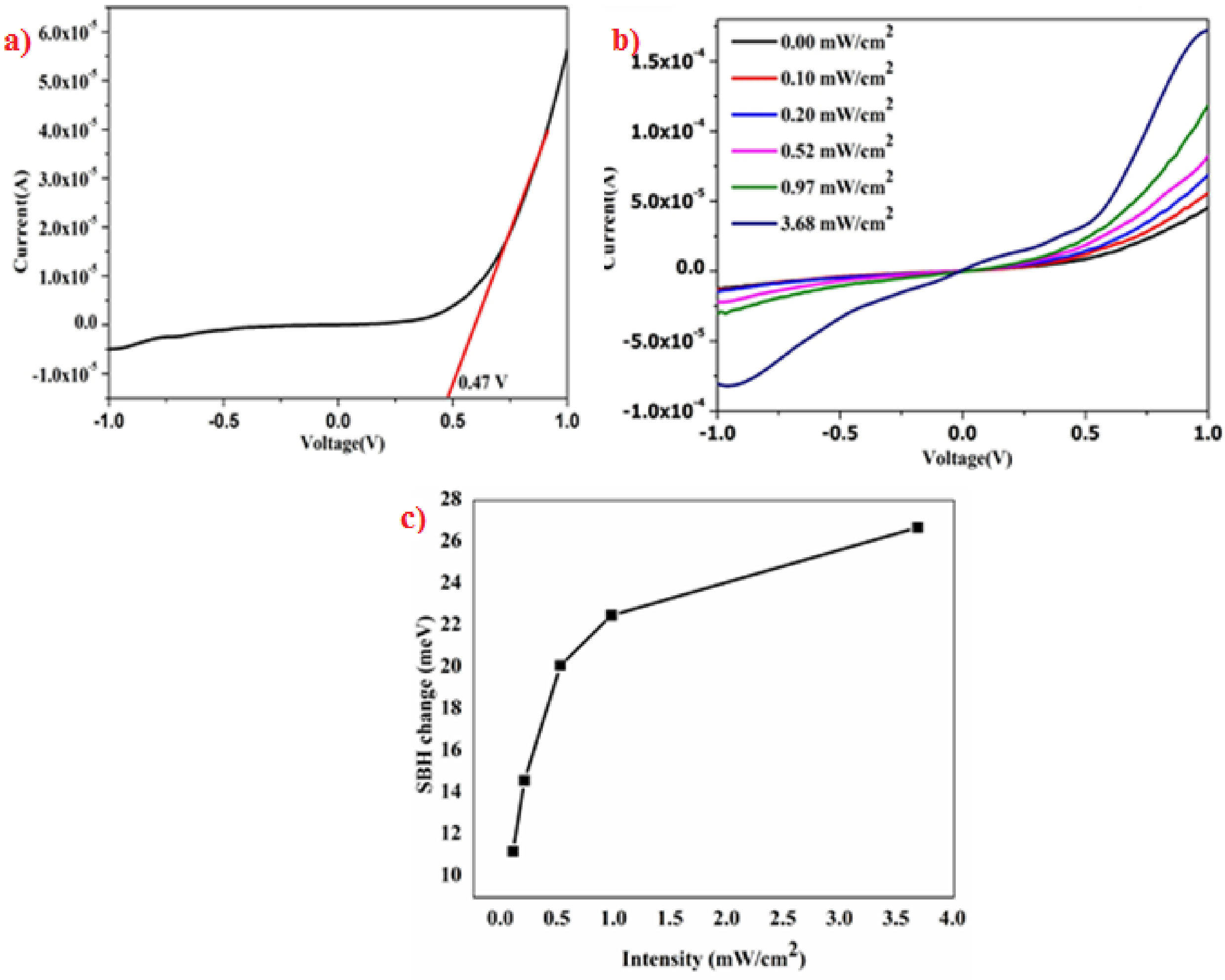


Figure 4: a) I-V characteristics of Pyrotronic diode b) I-V characteristics of Pyrotronic diode under different NIR illuminations c) Change in barrier height under different light illumination

In order to experimentally verify the development of pyroelectric nanogenerator based self-powered NIR photodetector, Gr/ZnO heterojunction without any external biasing was illuminated from ZnO end. Figure 4a shows the corresponding temporal response upon NIR illumination wherein as soon as the illumination is turned “ON’”, decrement in the current is observed. The decrement in the current can be attributed to the NIR light induced pyro-potential ($\Phi_{py}$) in the direction of barrier potential ($\Phi_b$) which cause the depletion region width to increase. Therefore, the total electric field inside the heterojunction increases instantly, and the time variation of the electric field leads to the flow of electrons thereby producing displacement current in the heterojunction which flows as short circuit output current through the external circuit as shown in figure 5d. After some time, the temperature difference becomes constant and hence current increases to its initial value. When the NIR illumination is turned off, increment in the current is observed which was due to the reverse pyro-potential generated in the direction opposite to that of barrier potential. Therefore, the depletion width shrinks and hence the total electric field inside the heterojunction decreases instantly, and the time variation of the electric field leads to the flow of electrons thereby producing displacement current in the heterojunction which flows as a short circuit output current through external circuit as shown in figure 5e. The same procedure was repeated for 6 times and similar response was observed. Figure 5b shows one such cycle representing the fall and rise of current on turning "ON" and "OFF" the NIR illumination. Rise time, defined as the time taken by the sensor to reach from 10% to 90% of its maximum value, was calculated to be 90 ms and the fall time was calculated to be 78 ms. The slow transient after the pyro peak current is reached can be attributed to the decrease in the temperature gradient (dT/dt) value which slows down the current response. When the NIR illumination is switched "ON" the temperature gradient (dT/dt) value is high i.e. the rate of change of temperature with time is high and hence a fast response was achieved, but as the NIR illumination is turned "ON" for a longer period, the temperature gradient (dT/dt) eventually becomes less and temperature eventually become constant and hence there is a slow response observed. It is clear that the decrease and increment of current occurs at zero bias due to the time varying field generated due to the repeated NIR illumination and hence hold tremendous potential as self-powered NIR photodetector. It should be noted here that there is no generation of photo carriers unlike in most of the conventional photodetectors, wherein the illumination leads to the photogenerated carriers which transport to the metal contact thereby increasing/decreasing the current. Herein, the current variation due to the NIR illumination occurs due to the pyro-potential generation which modulates the depletion region and not due to the photogenerated carriers. Also, graphene is known to respond to NIR illumination and generate photogenerated carriers [13], but in this case, NIR illumination was focused only on ZnO and hence Gr cannot generate the photogenerated carriers. This was done so as to avoid the accumulation of charge carriers inside the Gr as the work function of Gr is less than the electron affinity of ZnO which does not allow the photogenerated carriers from Gr to transport to ZnO. Hence photogenerated charge carriers would be trapped in Gr which would lead to the failure of device.

Responsivity is an important figure of merit of the photodetector and is given by the measure of the photocurrent generated per unit power of incident light area and is given by

$$R_\lambda = \frac{I_\lambda}{P_\lambda \times A}$$

Where $I_\lambda$ is the different of the photocurrent and dark current is, $P_\lambda$ is the intensity of the light illumination and A is the area of the device. The responsivity calculated for the fabricated device was found to be 2.64 $mW/cm^2$. Further, to test the reliability and robustness of the fabricated device, bending cycles studies were performed where the device was bend and bought to its initial position for 500 cycles and then responsivity values were measured. There was a small change in the values of responsivity observed at various bending cycles which can be attributed to the defects introduced during hydrothermal growth of 2D ZnO which upon bending results in the permanent deformations which affects the responsivity values.

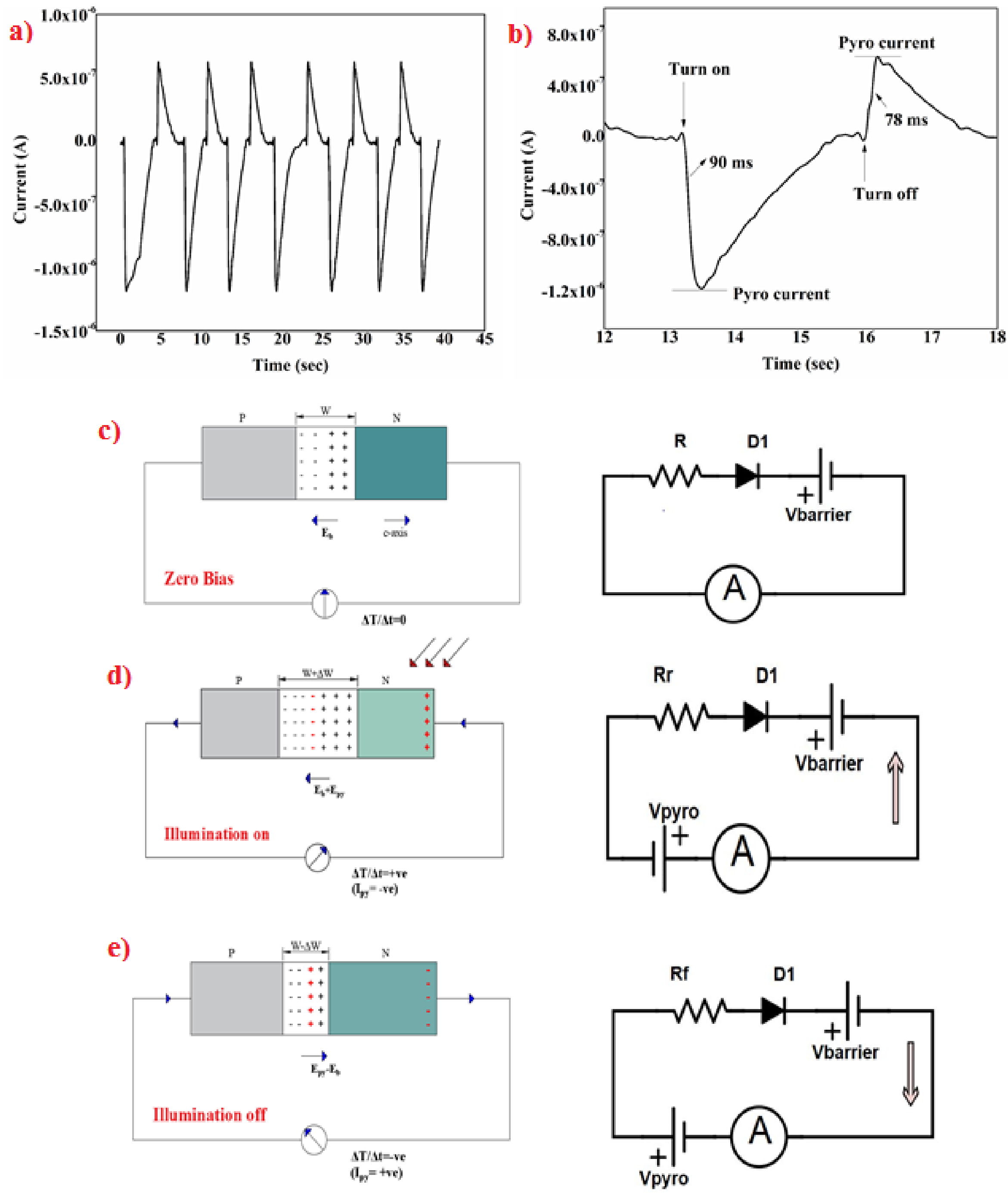


Figure 5: a) Temporal response of Pyrotronic diode under time varying NIR illumination b) One cycle of temporal response of Pyrotronic diode under time varying NIR illumination showing rise time of 90 msec c,d,e) Schematics showing the transport mechanism with and without illumination of Pyrotronic diode.

To further demonstrate the potential application of the fabricated heterojunction which can modulate the depletion width upon NIR illumination, it was utilized as a variable capacitor whose capacitance can be modulated upon NIR illumination in developing frequency modulator circuit. Schematic of the frequency modulator circuit is as shown in figure 5a. It consists of an amplifier circuit having coupling capacitances, bypass capacitances, biasing resistors and transistor (BC547) and feedback LC resonant circuit. The frequency of oscillation was observed in digital oscilloscope. The feedback capacitor was replaced by Gr/ZnO heterojunction. The frequency of oscillation of LC resonant circuit is given by,

$$f = \frac{1}{2\pi\sqrt{LC}}$$

To obtain the sustained oscillation, gain of the amplifier was adjusted. Gr/ZnO heterojunction forms a barrier potential or depletion region which can act as a capacitor. Under no illumination, frequency of oscillation was found to be 9.8 MHz. Figure 5b shows the graph of different frequencies generation upon illumination intensity of 1.81 mW/cm$^2$and it was observed that both frequency and Vpeak-peak modulates. This can be attributed to the modulation of the depletion region width upon NIR illumination. Upon NIR illumination from ZnO side, pyro-potential generated sums up with barrier potential and hence the depletion region width increases which decreases the junction capacitance and hence frequency of oscillation increases. As the temperature difference becomes constant, pyro potential vanishes and the frequency of oscillations retains its initial value. As soon as the NIR illumination is turned “OFF”, pyro-potential is induced in opposite direction and hence the depletion region width decreases which increases the capacitance and decreases the frequency of oscillation. Hence time varying NIR illumination can be utilized for frequency modulation. Figure 5c shows the graph of maximum frequency of oscillation achieved upon turning “ON” the illumination of different NIR intensities suggesting that as the illumination intensity increases the maximum frequency of oscillation increases. Further, peak to peak voltage (Vpp) of the oscillation was monitored and it was found that upon turning “ON” the illumination, the Vpp of the oscillation also increases with increase in the illumination intensity. This can be attributed to the addition of both pyro and barrier potential which increases the Vpp of the oscillation. Figure 5d shows the graph of Vpp and maximum Fosc under different NIR illumination intensities. It should be noted that the frequency of light modulation was not in MHz. The change in the frequency of oscillations depends upon the change in the capacitance value of the pyrotronic diode and hence when light was repeatedly turned “ON” and “OFF” the pyro potential generated increases the width of the depletion region and hence the capacitance decreases. This decrease in the capacitance leads to the increase in the frequency of oscillations. Also, the measurements were not performed for different wavelengths of NIR region because the reason for choosing NIR illumination was to induce temperature difference. However, to induce temperature difference, different intensities at 780 nm wavelength were utilized for measurements.

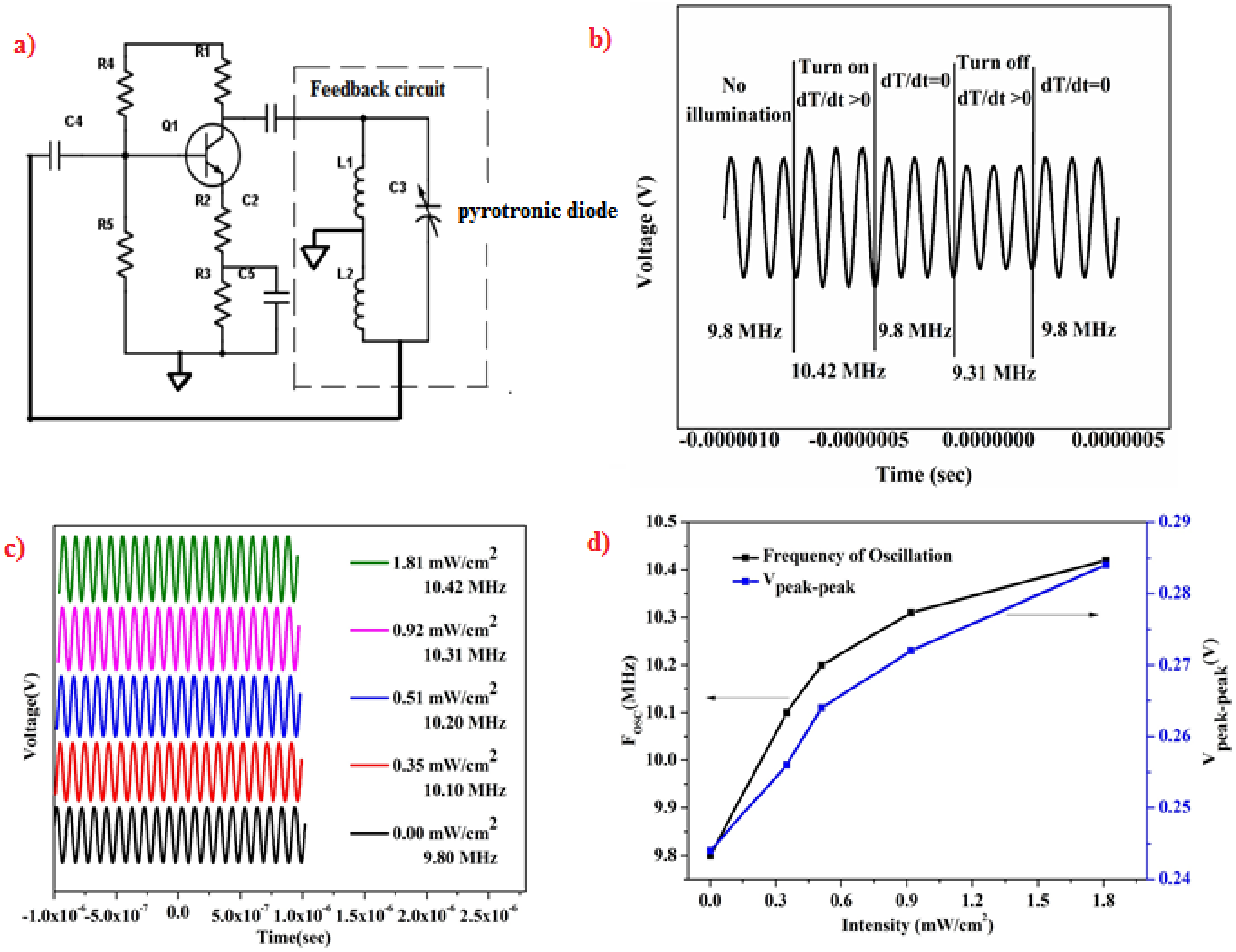


Figure 6: a) Schematic of frequency modulator circuit with Pyrotronic diode as capacitor b) Frequency modulation response under 1.81 mW/cm2 NIR illumination intensity c) Frequency modulation with different intensities showing only ON state frequencies d) Graph showing the variation of frequency of oscillation and Vpeak-peak with different NIR intensities.

The phenomena of pyro-potential generation and the modulation of the depletion region and further utilizing it for frequency modulator can be better understood by energy band diagram of the Gr/ZnO Pyrotronic diode as shown in figure 7. The work function of Gr is 4.365 eV

[14] and the electron affinity of ZnO is 4.3 eV [8] and the bandgap of ZnO is 2.8 eV. The reason for barrier height value to be different from the theoretical values can be attributed to the oxidation of Gr in ambient atmosphere. Upon turning "ON" the NIR illumination from ZnO side, pyro-potential is generated which is in same direction to that of barrier potential and hence the effective barrier height increases as shown in figure 7. The pyro-potential is a function of time and hence when the temperature difference becomes constant, the pyro-potential vanishes since the potential observed by the heterojunction would only be barrier potential. Upon turning off the NIR illumination, reverse pyro-potential is generated which is in opposite direction to that of barrier potential and the effective barrier height decreases. Eventually the temperature difference becomes constant and hence the reverse pyro-potential vanishes and again the potential observed by the heterojunction would only be barrier potential. Moreover, heterojunction possess junction capacitance whose value depends upon the width of the depletion region and modulation of depletion region width would also modulate the junction capacitance of the heterojunction which could be applied for realizing various analog circuits.

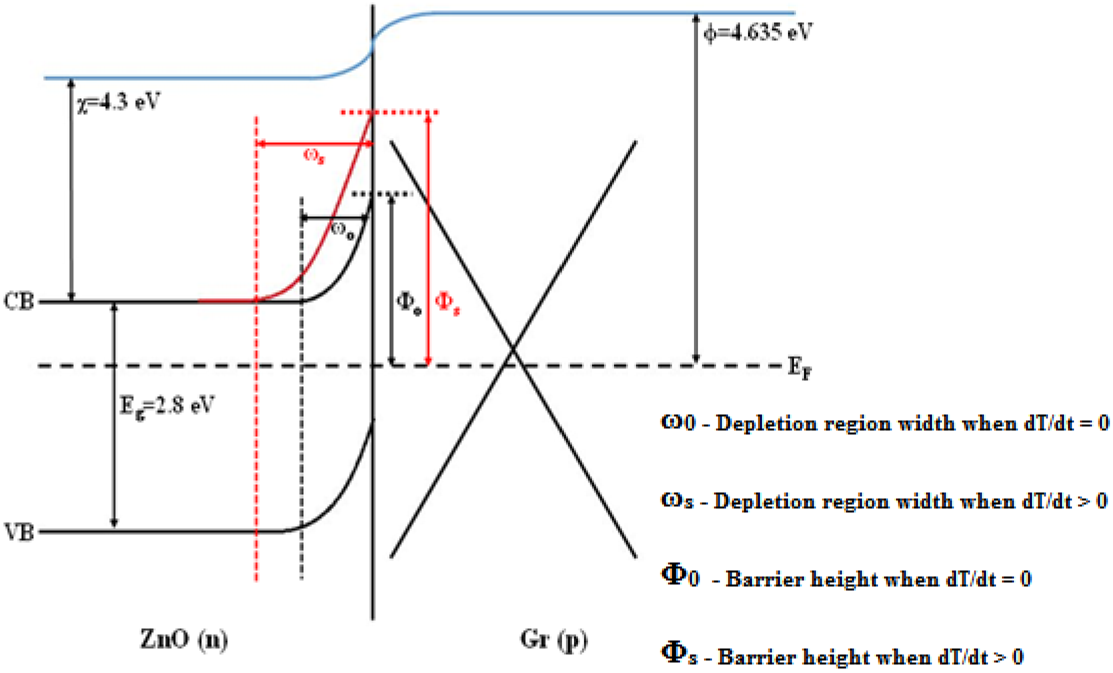


Figure 7: Energy band diagram of Pyrotronic diode with and without NIR illumination

There are various reports on self-powered photodetectors based on functional materials that are based on techniques such as piezoelectricity, photovoltaics, and recently studied triboelectricity. [15-16] More recently, a different technique that is recently being studied is pyroelectricity. There are reports on pyroelectricity being explored for its use in self-powered photodetectors. *Wang et al.*, utilized ZnO for light induced pyroelectric effect as ultraviolet sensing which increased the performance of photodetector in terms of rise time and detectivity. [3] *Wang et al.*, reported light induced pyroelectric nanogenerator for self-powered infrared sensing [17]. Table showing the comparative performance of the fabricated photodetector in terms of responsivity can be found in SI as table S1. But the use of such heterojunctions for the development of real time analog circuits such as oscillator and frequency modulators still remains unexplored and is important in interactive flexible and wearable electronic applications. In this paper we report the fabrication of flexible Pyrotronic diode using Gr/ZnO on an ITO coated PET substrate which was utilized as a variable capacitor in frequency modulator circuit. The fabrication cost is considerably less compared to cleanroom fabricated devices due to the solution processed technique. The synthesis strategy allows for large area growth and can be extended to any many other functional materials of choice. This low cost, large area fabrication of flexible Gr/ZnO Pyrotronic diode is a novel concept that finds numerous applications in biomedical, optothermal detections and in developing interactive analog electronic devices.

## 3.4 Conclusion

In summary, this work represents the first demonstration for fabrication of Pyrotronic diode and its application in self-powered NIR photodetector and active analog frequency modulation. Ideality factor and barrier height calculated for Pyrotronic diode was found to be 1.97 and 0.357 eV which is excellent considering the simplicity of the device fabrication. Upon light illumination, maximum barrier height change of 27 meV was observed which increased the depletion region width which results in the decrease in the junction capacitance. This variation in junction capacitance upon light illumination was further utilized for analog frequency modulator wherein frequency change from 9.8 MHz to 10.42 MHz was observed. This simple, cost-effective fabrication of Pyrotronic diode is a major step ahead in the development of self-powered devices which can be used for interactive electronic devices having potential applications in the field of optothermal imaging, optoelectronics and sensors.

Acknowledgement

The authors acknowledge the financial assistance from Defense Research and Development Organization (DRDO), India Grant ERIP/ER/RIC/2015-6/10/M/01/1660 and seed grant, IIT Hyderabad.

## 3.5 References

1. Sahatiya, P., & Badhulika, S. Fabrication of a solution-processed, highly flexible few layer MoS 2 (n)–CuO (p) piezotronic diode on a paper substrate for an active analog frequency modulator and enhanced broadband photodetector. *Journal of Materials Chemistry C*, **2017**.
2. Zhou, T., Yang, Z. W., Pang, Y., Xu, L., Zhang, C., & Wang, Z. L. Tribotronic tuning diode for active analog signal modulation. *ACS Nano*, **2016**, 11(1), 882-888.

3. Wang, Z., Yu, R., Pan, C., Li, Z., Yang, J., Yi, F., & Wang, Z. L. Light-induced pyroelectric effect as an effective approach for ultrafast ultraviolet nanosensing. *Nature Communications*, **2015**, 6, 8401.
4. Sahatiya, P., & Badhulika, S. One-step in situ synthesis of single aligned graphene–ZnO nanofiber for UV sensing. *RSC Advances*, **2015**, 5(100), 82481-82487.
5. Veerla, R. S., Sahatiya, P., & Badhulika, S. Direct writing of ZnO pencil on paper based flexible UV photodetector and disposable Photoresponsive Uric Acid sensor. *Journal of Materials Chemistry C*, **2017**, 5, 10231-10240
6. Wang, Z. L., &Song, J. Piezoelectric nanogenerators based on zinc oxide nanowire arrays. *Science*, **2006**, 312(5771), 242-246.
7. Dang, V. Q., Trung, T. Q., Kim, D. I., Duy, L. T., Hwang, B. U., Lee, D. W., & Lee, N. E. Ultrahigh responsivity in graphene–ZnO nanorod hybrid UV photodetector. *Small*, **2015**, 11(25), 3054-3065.
8. Sahatiya, P., Jones, S. S., Gomathi, P. T., & Badhulika, S. Flexible substrate based 2D ZnO (n)/graphene (p) rectifying junction as enhanced broadband photodetector using strain modulation. *2D Materials*, **2017**, 4(2), 025053
9. Hwang, J. O., Lee, D. H., Kim, J. Y., Han, T. H., Kim, B. H., Park, M., & Kim, S. O. Vertical ZnO nanowires/graphene hybrids for transparent and flexible field emission. *Journal of Materials Chemistry*, **2011**, 21(10), 3432-3437.
10. Chung, K., Lee, C. H., & Yi, G. C. Transferable GaN layers grown on ZnO-coated graphene layers for optoelectronic devices. *Science*, **2010**, 330(6004), 655-657.
11. Zhang, F., Niu, S., Guo, W., Zhu, G., Liu, Y., Zhang, X., & Wang, Z. L. Piezo-phototronic effect enhanced visible/UV photodetector of a carbon-fiber/ZnO-CdS double-shell microwire. *ACS Nano*, **2013**, 7(5), 4537-4544.
12. Zhou, J., Gu, Y., Fei, P., Mai, W., Gao, Y., Yang, R., & Wang, Z. L. Flexible piezotronic strain sensor. *Nano Letters*, **2008**, 8(9), 3035-3040.
13. Sahatiya, P., Puttapati, S. K., Srikanth, V. V., & Badhulika, S. Graphene-based wearable temperature sensor and infrared photodetector on a flexible polyimide substrate. *Flexible and Printed Electronics*, **2016**, 1(2), 025006.
14. Shi, Y., Kim, K. K., Reina, A., Hofmann, M., Li, L. J., & Kong, J. Work function engineering of graphene electrode via chemical doping. *ACS Nano*, **2010**, 4(5), 2689-2694.
15. Zhang, C., Zhang, L. M., Tang, W., Han, C. B., & Wang, Z. L. Tribotronic logic circuits and basic operations. *Advanced Materials*, **2015**, 27(23), 3533-3540.

16. Wu, W., Wei, Y., & Wang, Z. L.Strain-Gated Piezotronic Logic Nanodevices. *Advanced Materials*, **2010**, 22(42), 4711-4715.
17. Wang, X., Dai, Y., Liu, R., He, X., Li, S., &Wang, Z. L. Light-Triggered Pyroelectric Nanogenerator Based on a pn-Junction for Self-Powered Near-Infrared Photosensing. *ACS Nano*, **2017**, 11(8), 8339-8345.
18. Sahatiya, P., Shinde, A., & Badhulika, S. (2018). Pyro-phototronic nanogenerator based on flexible 2D ZnO/graphene heterojunction and its application in self-powered Near Infrared photodetector and active analog frequency modulation. *Nanotechnology*.

# Chapter 4

# Wireless smartphone assisted personal healthcare monitoring system using $MoS_2$ based flexible, wearable and ultra-low cost multifunctional sensor

**Abstract—** Flexible, wearable, multifunctional sensors that can quantify electrical signals generated by human activities are of great importance in personal healthcare monitoring for Internet of Things (IoT) applications. In this report, we demonstrate for the first time, the multifunctionality of $MoS_2$ grown on Al foil and further integrated onto eraser substrate to develop smart, low cost pedometer, gesture communication device and breath sensor by measuring physiological parameters such as strain, touch, hydration levels of lungs respectively. The data generated is wirelessly transmitted to the smartphone via Bluetooth and analysed using dedicated android applications for individual sensing displays. For pedometer, the fabricated sensor was integrated onto the knee which could then calculate the steps taken, distance covered, speed and the calories burnt by the individual. Gesture communication helps the deaf/dumb/paralyzed individuals to communicate with external environment using finger movements. Breath sensing allows for the early detection of lung diseases by monitoring the hydration levels of the lungs and further the piezotronic effect of $MoS_2$ on breath sensing was systematically studied where 56.8% increase in the response was observed under 16% strain. The sensing mechanism for each stimulus is explained via modulation in the charge transport properties for each stimuli. The sensor exhibited excellent durability where the device performance was found to be stable even after continuous 500 bending cycles. The successful demonstration of such low cost multifunctional wireless personal healthcare monitoring

system for Internet of Things (IoT) applications is a major step ahead in flexible and wearable electronics.

## 4.1 Introduction

Advancements in flexible and wearable electronics have opened up new avenues in personal healthcare development that can monitor the individual physiological parameters continuously or at a regular intervals and thus act as reliable indicators in early disease diagnostics [1-2]. These existing technologies in health care however rely mostly on use of sophisticated and specialized sensors, instruments and services thereby leading to an increase in the overall cost of healthcare. Moreover, to access these facilities, individual need to visit hospital and clinics which is not only tedious but also costly. There are recent reports on personal health monitoring which utilize physiological parameters of an individual for glucose monitoring through tears, human motion monitoring, breath sensing for lung disease etc [3-5]. However, there are few reports which utilizes the low cost sensors for multifunctional sensing wherein the data can be wirelessly transmitted to smartphone with a dedicated android application for individual sensing [6]. Hence there is an urgent need for constant personal health monitoring system with wearable sensors which can monitor parameters such as breath, human motion, human steps (pedometer) and the data can be transferred to the smartphone for a convenient read-out.

To fabricate multifunctional sensor, functional nanomaterials are utilized as active elements which respond to different chemical stimuli thereby leading to the overlap of the sensor data. To address this, various frontend processing algorithms such as principal component analysis and pattern recognition have been applied to the sensing data but these often lead to unreliable data [7-8]. Moreover, there is always a question on reliability and accuracy of the multifunctional sensor because of the utilization of the same sensor for different applications. Hence, flexible, ultra-low cost sensors are the ideal choice wherein different sensors can be fabricated with the same functional nanomaterial for individual sensing with an ability to transfer the sensing data to smartphone with a dedicated android application.

In this work we develop a low cost wireless personal monitoring system using solution processed $MoS_2$ grown on Al foil as an active sensing element with a dedicated android application for multi parameters sensing. The proposed system can be utilized as a pedometer for calculating the number of walking/running steps and the calories burnt, breath sensor for monitoring breath of an individual, and a hand gesture communication sensor for paralyzed patients. Further each system consists of a dedicated android mobile application which receives the sensor data wirelessly through Bluetooth and displays the information regarding distance travelled, velocity, calories burnt for pedometer module, breath count for breath sensor module and action related to a specific gesture for gesture communication sensor module. To the best of author's knowledge this is the first demonstration of $MoS_2$ grown on Al foil for wireless personal healthcare monitoring IoT system (pedometer, gesture communication and breath sensing) with dedicated Android application for each sensing module.

## 4.2 Results and discussions

### Pedometer

A pedometer is an electronic device that counts steps taken by an individual by detecting the motion of the individual hands or knees. This can be further utilized for the calculation of the distance travelled, velocity and calories burnt. Even though there are numerous Android applications that have been developed for fitness monitoring [13-14], these applications work without the integration of a sensor and demands the user to continuously update the information. Moreover, without the use of a dedicated sensor, the data from the application is not reliable which results in the falsified data. Hence there is a need to develop sensor with a dedicated Android application where the data from the sensor can be continuously transmitted wirelessly to the smartphone. . Further, the measurements were also performed by measuring the response through the Arduino board and transmitting the data wirelessly via Bluetooth to smartphone. Figure 2e shows the digital images of the Android application that was developed for $MoS_2$/Al foil based pedometer which displays the distance travelled, velocity and calories burnt.

### Gesture Recognition

Motivated by the response of $MoS_2$/Al to strain variations, the fabricated sensor was further utilized as a gesture sensor which will be of immense benefit to paralyzed/dumb subjects in communicating with the outside world. Traditional human machine interactions (HMI) include hand operation, speech input etc. whereas bioelectric signals include electroencephalogram (EEG), electromyogram (EMG) and electrooculogram (EOG) which are non-invasive and have the advantage of hands free communication [15-16]. But such signals require sophisticated instrumentation and dedicated skilled labour for its operation which not only increases the cost of the system but also increases the complexity and the dependency of the patient on various external factors. Further low signal to noise ratio limits the use of such systems in real time. Deaf and dumb people face difficulties in communicating for availing daily necessary things such as food, communicating for different needs etc. Hence there is an urgent need to develop gesture sensor which is wirelessly connected to the smartphone with a dedicated android application which takes cares not only of the daily needs of such patients but also helps to communicate easily with the other people. The corresponding selection is wirelessly transmitted to the other individuals (doctor, family etc.) and the necessary action can be taken. Figure 3b shows the response of the sensor integrated onto human finger and its corresponding movement. As the finger is bent inwards, tensile strain is developed on eraser which gets transferred to $MoS_2$/Al foil thereby changing the resistance of the $MoS_2$/Al foil. The mechanism for the change in resistance of $MoS_2$/Al upon bending is based on tunneling resistance change similar to pedometer sensing as explained in previous section.

**Breath Sensing**

Point of care devices have become an integral part of human life because of their ability to detect several vital body parameters and early stages of diseases [17-18]. There have been reports on monitoring of blood pressure, glucose levels and pregnancy etc. whose sensing data can be wirelessly transmitted to the smartphone [19-20]. Human breath is another such metric whose sensing/analysis can lead to the detection of early stages of several diseases. The humidity sensing of $MoS_2$/$Cu_2S$ and its further utilization as breath sensing to monitor the hydration levels of the lungs was recently reported by our lab [6]. But still there is a lot of scope for the exploration of breath sensing for detection of various lung disease and hence there is an urgent need for wireless breath monitoring/sensing system. Odd layer of $MoS_2$ are known to exhibit piezoelectric behavior because of the non-centrosymmetric alignment of Mo and S atoms [21]. There have been reports to enhance the sensitivity of the sensor by utilizing the piezo property of $MoS_2$ [22], percentage of relative humidity [6]. whereas current level of the sensor tries to reach initial value during the inhalation. 12 breath counts per 30 second were observed under normal breath conditions which is a sign of a healthy individual. To test the repeatability of the fabricated sensor, the individual was asked to breath and then move away from the sensor and this cycle was repeated for 6 times. The sensor was able to detect the modulation in breath shown in figure 4b. Further, the individual was asked to run continuously for 20 minutes and was asked to relax for a minute so as to stabilize the breath pattern and then breath sensing measurements were performed.

The sensing mechanism for pristine $MoS_2$ under breath sensing can be explained as the resistance modulation upon subject's breath modulation due to the absorption of water molecules on $MoS_2$/Al in exhaled breath. Exhaled breath contains water molecules (moisture) and the amount of moisture depends on the hydration level of the lungs. Upon exhalation, the water molecules which are electron donating in nature get adsorbed on $MoS_2$ (n type), thereby increasing the majority charge carriers in $MoS_2$ which increases the current level of $MoS_2$. During inhalation, the water molecules desorb from the surface of $MoS_2$ and hence the current level decreases and tries to retain its initial values. It should be noted that due to the slow desorption process, the current level does not regain entirely its initial value, but is not critical as the number of peaks corresponds to the number of breath counts. The same concept can be explained using energy band diagram of $MoS_2$ where there is a downward bending at the $MoS_2$/metal interface upon adsorption of water molecule during thereby allowing the easy flow of electrons towards the metal contact which increases the current.

**Wireless integration of sensor**

The fabricated $MoS_2$/Al on eraser was interfaced with Arduino microcontroller and further the data received was transmitted to the smartphone wirelessly via Bluetooth. The dedicated android application was developed wherein individual modules were utilized for each sensing such as breath, gesture and pedometer. Figure 5a displays the schematic of the circuit diagram of the interfacing of $MoS_2$/Al sensor with Arduino Uno board and wireless transmission to the smartphone via a Bluetooth. Simple resistance divider circuit was utilized for measuring the resistance of the sensor. Bluetooth module (HC-05) which uses easy serial port protocol for transparent wireless serial connection setup was utilized to transmit the data from Arduino to smartphone wirelessly. An android application was developed for receiving the sensor's real time data and to display related results about breath, gesture and pedometer on the smartphone. Figure 5b shows the frontend display of the android application which consists of three modules namely Pedometer, Hand Gesture and Breath sensing. The user can select the dedicated module and perform the corresponding sensing. Figure 5 c, d e shows the corresponding real time sensor data acquired by the smartphone for pedometer, gesture and breath sensing respectively. The data was acquired and monitored on frontend of the android application by continuously varying the respective stimuli.

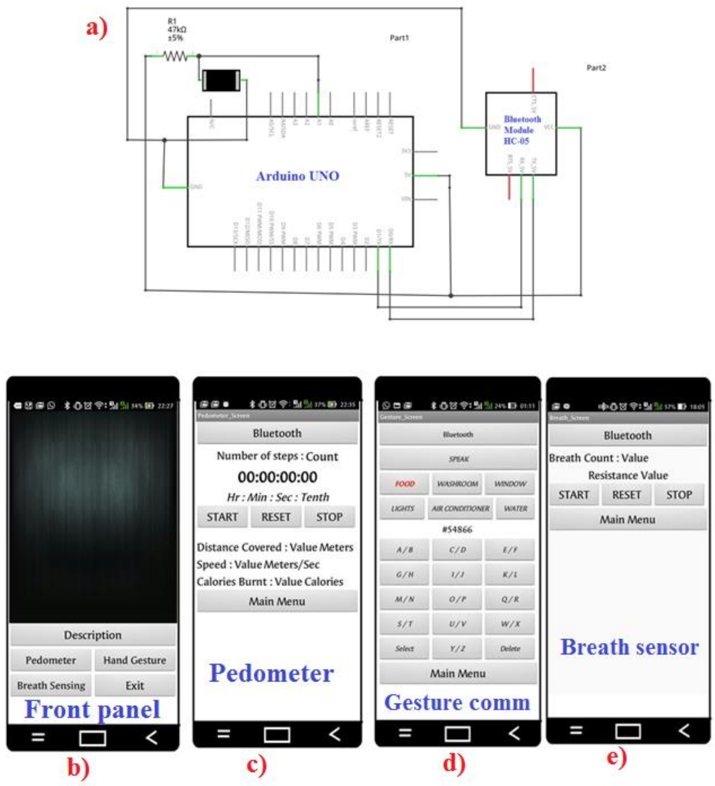


**Figure 5**: a) Schematic of the circuit diagram utilized for the integration of MoS2/Al sensor with Arduino microcontroller, Digital snapshot of b) front screen of the Android application developed for personal healthcare monitoring c) for pedometer module d) gesture communication module and e) breath sensing module

There are few reports for smartphone based point of care diagnostic of early disease using various stimuli such as glucose, sweat, saliva etc. *Bhattacharjee et al.*, demonstrated wireless breath sensor which detects the humidity of the lungs [23]. *Dang et al.*, reported the novel graphite-polyurethane composite for wireless system for pH monitoring [24]. *Kakehi et al.*, developed wireless glucose monitoring system which could be operated stably for 3 days [25]. *Pu et al.*, developed self-powered triboelectric gesture sensor based on the eyes movement

[26]. All these reports however focus on individual sensing and thus are limited in their scope of applications which is crucial for IoT applications. There are existing reports on multifunctional sensors which use the same fabricated sensor for individual sensing and apply complicated frontend processing which often results in unreliable data. Moreover, the fabrication techniques employed for these sensors are sophisticated which makes the overall cost of production unfit for developing affordable flexible and wearable IoT systems. Further, the utilization of the same sensor for sensing different entities always results in falsified data. There are no reports on multifunctional sensing utilizing dedicated sensor and android application for each sensing. In this report, we demonstrate the fabrication of wireless multifunctional sensor which could be utilized as pedometer, gesture communication and breath sensor for diagnosing various disease. The cost of each sensor is ~ $0.015 and hence allows the user to utilize dedicated sensor for individual sensing.

### 4.3 Conclusion

In summary, we demonstrate the use of $MoS_2$ grown on Al foil and integrated onto eraser substrate for its utilization as personal healthcare monitoring (pedometer, gesture communication and breath sensor) for IoT applications. The sensor was integrated with Arduino microcontroller wherein the sensor data was wirelessly transmitted to the smartphone. Dedicated android application was developed for pedometer, gesture communication and breath sensor wherein the pedometer module provides information about the distance travelled, speed and the calories burnt. The gesture communication modules helps the deaf/dumb/paralyzed individuals to communicate with the external world using the hand finger movements. Breath sensor module provides information regarding breath pattern which could be further utilized for many personal healthcare applications. Further, the piezotronic effect of $MoS_2$ under external strain of 16% on the breath sensing performance was studied which results in 56.89 % enhanced sensing when compared to breath sensing performance of unstrained $MoS_2$. The successful development of such multifunctional, user friendly wireless sensors are a major step ahead in flexible and wearable IoT applications such as personal healthcare monitoring.

## 4.5 References


1. Emaminejad, S., Gao, W., Wu, E., Davies, Z. A., Nyein, H. Y. Y., Challa, S., & Talebi, S. Autonomous sweat extraction and analysis applied to cystic fibrosis and glucose monitoring using a fully integrated wearable platform. *Proceedings of the National Academy of Sciences*, **2017**, pp: 201701740.
2. Geldert, A., Zhang, X., Zhang, H., & Lim, C. T. Highly sensitive and selective aptamer-based fluorescence detection of a malarial biomarker using single-layer MoS2 nanosheets. *ACS Sensors*, **2016**, vol. 1, pp: 1315
3. Yao, H., Shum, A. J., Cowan, M., Lähdesmäki, I., & Parviz, B. A. A contact lens with embedded sensor for monitoring tear glucose level. *Biosensors and Bioelectronics*, **2011**, vol. 26, pp:3290.
4. Sahatiya, P., & Badhulika, S. Eraser-based eco-friendly fabrication of a skin-like large-area matrix of flexible carbon nanotube strain and pressure sensors. *Nanotechnology*, **2017**, vol.28, pp: 095501.
5. Di Natale, C., Macagnano, A., Martinelli, E., Paolesse, R., D'Arcangelo, G., Roscioni, C., & D'Amico, A. Lung cancer identification by the analysis of breath by means of an array of non-selective gas sensors. *Biosensors and Bioelectronics*, **2003**, vol. 18, pp: 1209.
6. Sahatiya, P., Kadu, A., Gupta, H., Gomathi, P. T., & Badhulika, S. Flexible, disposable cellulose paper based $MoS_2$-$Cu_2S$ hybrid for wireless environmental monitoring and multifunctional sensing of chemical stimuli. *ACS Applied Materials & Interfaces*, **2018**, vol. 10, pp: 9048
7. Li, Y., Li, Y., Su, M., Li, W., Li, Y., Li, H., & Song, Y. Electronic Textile by Dyeing Method for Multiresolution Physical Kineses Monitoring. *Advanced Electronic Materials*, **2017**, vol. 3, pp: 1700253
8. Mantyjarvi, J., Himberg, J., & Seppanen, T. Recognizing human motion with multiple acceleration sensors. In Systems, Man, and Cybernetics, 2001 IEEE International Conference on (Vol. 2, pp. 747-752). IEEE.

9. Wang, D., Zhang, X., Bao, S., Zhang, Z., Fei, H. and Wu, Z., Phase engineering of a multiphasic 1T/2H $MoS_2$ catalyst for highly efficient hydrogen evolution, *Journal of Materials Chemistry A*, **2017**, vol. 5, pp: 2681.
10. Gigot, A., Fontana, M., Serrapede, M., Castellino, M., Bianco, S., Armandi, M., Bonelli, B., Pirri, C.F., Tresso, E. and Rivolo, P., Mixed 1T–2H Phase $MoS_2$/Reduced Graphene Oxide as Active Electrode for Enhanced Supercapacitive Performance, *ACS applied materials & interfaces*, **2016**, vol. 8, pp: 32842.
11. Yun, J.M., Noh, Y.J., Lee, C.H., Na, S.I., Lee, S., Jo, S.M., Joh, H.I. and Kim, D.Y., Exfoliated and Partially Oxidized $MoS_2$ Nanosheets by One-Pot Reaction for Efficient and Stable Organic Solar Cells, *Small*, **2014**, vol. 10, pp: 2319.
12. Sahatiya, P., Jones, S. S., & Badhulika, S. Direct, large area growth of few-layered $MoS_2$ nanostructures on various flexible substrates: growth kinetics and its effect on photodetection studies. *Flexible and Printed Electronics*, **2018**, vol. 3, pp: 015002.
13. Su, X., Tong, H., & Ji, P. Activity recognition with smartphone sensors. *Tsinghua Science and Technology*, **2014**, vol. 19, pp: 235
14. Kranz, M., MöLler, A., Hammerla, N., Diewald, S., PlöTz, T., Olivier, P., & Roalter, L. The mobile fitness coach: Towards individualized skill assessment using personalized mobile devices. *Pervasive and Mobile Computing*, **2013**, vol. 9, pp: 203-215.
15. Birbaumer, N., Ghanayim, N., Hinterberger, T., Iversen, I., Kotchoubey, B., Kübler, A., & Flor, H. A spelling device for the paralysed. *Nature*, **1999**, vol. 398, pp: 297.
16. Chen, X., Wang, Y., Nakanishi, M., Gao, X., Jung, T. P., & Gao, S. High-speed spelling with a noninvasive brain–computer interface. *Proceedings of the National Academy of Sciences*, **2015**, vol. 112, pp: E6058.
17. Chin, C. D., Linder, V., & Sia, S. K. Commercialization of microfluidic point-of-care diagnostic devices. *Lab on a Chip*, **2012**, vol. 12, pp: 2118.
18. Wang, J. Electrochemical biosensors: towards point-of-care cancer diagnostics. *Biosensors and Bioelectronics*, **2006**, vol. 21, pp: 1887.
19. Mahato, K., Srivastava, A., & Chandra, P. Paper based diagnostics for personalized health care: Emerging technologies and commercial aspects. *Biosensors and Bioelectronics*, **2017**, vol. 96, pp: 246.
20. Bisio, I., Lavagetto, F., Marchese, M., & Sciarrone, A. Smartphone-centric ambient assisted living platform for patients suffering from co-morbidities monitoring. *IEEE Communications Magazine*, **2015**, vol. 53, pp: 34.

21. Huang, Y., Liu, L., Sha, J., & Chen, Y. Size-dependent piezoelectricity of molybdenum disulfide (MoS2) films obtained by atomic layer deposition (ALD). *Applied Physics Letters*, **2017**, vol. 111, pp: 063902.
22. Sahatiya, P., & Badhulika, S. Fabrication of a solution-processed, highly flexible few layer MoS2 (n)–CuO (p) piezotronic diode on a paper substrate for an active analog frequency modulator and enhanced broadband photodetector. *Journal of Materials Chemistry C*, **2017**, vol. 5, pp: 11436.
23. Bhattacharjee, M., Nemade, H. B., & Bandyopadhyay, D. Nano-enabled paper humidity sensor for mobile based point-of-care lung function monitoring. *Biosensors and Bioelectronics*, **2017**, vol. 94, pp: 544.
24. Dang, W., Manjakkal, L., Navaraj, W. T., Lorenzelli, L., Vinciguerra, V., & Dahiya, R. Stretchable Wireless System for Sweat pH Monitoring. *Biosensors and Bioelectronics*, **2018**. DOI: 10.1016/j.bios.2018.02.025
25. Kakehi, N., Yamazaki, T., Tsugawa, W., & Sode, K. A novel wireless glucose sensor employing direct electron transfer principle based enzyme fuel cell. *Biosensors and Bioelectronics*, **2007**, vol. 22, pp: 2250.
26. Pu, X., Guo, H., Chen, J., Wang, X., Xi, Y., Hu, C., & Wang, Z. L. Eye motion triggered self-powered mechnosensational communication system using triboelectric nanogenerator. *Science Advances*, **2017**, vol. 3, pp: e1700694